Improvement of Elevation Model Accuracy and Suitability for Hydrodynamic Modelling

Prangya Paramita Sarkar
March, 2009

Course Title:	Geo-Information Science and Earth Observation for Environmental Modelling and Management
Level:	Master of Science (Msc)
Course Duration:	September 2007 - March 2009
Consortium partners:	University of Southampton (UK) Lund University (Sweden) University of Warsaw (Poland) International Institute for Geo-Information Science and Earth Observation (ITC) (The Netherlands)
GEM thesis number:	2007-22

Improvement of Elevation Model Accuracy and Suitability for Hydrodynamic Modelling

by

Prangya Paramita Sarkar

Thesis submitted to the International Institute for Geo-information Science and Earth Observation in partial fulfilment of the requirements for the degree of Master of Science in Geo-information Science and Earth Observation for Environmental Modelling and Management

Thesis Assessment Board

Chairman:	Prof. Dr. V.G. (Victor) Jetten
External Examiner:	Prof. Kasia Dabrowska-Zielinska
Internal Examiner:	Dr. Dinand Alkema
Supervisor:	Dr. Norman Kerle
Supervisor:	Dr. M.W. (Menno) Straatsma

ITC International Institute for Geo-Information Science and Earth Observation
Enschede, The Netherlands

Disclaimer

Abstract

Flooding is one of the most destructive and frequent natural disasters affecting many countries of the world. Increasing precipitation due to climate change is increasing the probability of related phenomena such as floods in future. Thus, there is a need of efficient flood risk management. Flood models have a great potential to aid flood risk management. The most important component of flood models is the surface elevation information. The efficiency of prediction about different derivatives of water flow during a flood event depends upon the elevation information. Thus, for flood event analysis and flood risk management, the elevation information should be accurate.

Photogrammetrically derived elevation models represent the earth's surface topography along with the surface features on it. Some of the surface features are impermeable obstacle to water flow (e.g. buildings) and some of them are permeable (e.g. trees). The presence of actually impermeable obstacles in the elevation model can influence the flow of water and thus can make the flood model prediction erroneous. Therefore, those impermeable obstacles should be eliminated from the elevation model and the permeable obstacles should be retained there.

From this motivation the present study was undertaken to develop a semi-automatic method to remove the impermeable obstacles and retain the permeable obstacles in the photogrammetrically derived surface model. This research used scanned coloured aerial photo to generate a digital surface model (DSM) and orthophoto of the study area. The method was formulated, firstly, to identify the features and secondly, remove relevant features selectively from the DSM. Only pixel based analysis was taken into consideration to limit the scope of the study. Colour and texture of the landcover features were used to identify the features. Binarisation-interpolation method and neighbourhood analysis were used to remove the relevant features from the DSM. The resultant elevation model is termed as pseudo-DTM. Later on the pseudo-DTMs obtained through different methods were compared with a reference LiDAR DTM to assess their precession and accuracy. The methods were also assessed with respect to different practical scenarios.

The present research proposes two different methods for selective removal of the surface features from the DSM. This research is a stepping stone for further exploration in this field using similar technique but with more detailed dataset.

Acknowledgements

I would like to express my thanks to the European Union and the Erasmus Mundus consortium (University of Southampton, UK, Lund University, Sweden, Warsaw University, Poland and ITC, the Netherlands) for awarding me the scholarship and giving me the opportunity to gain knowledge from the esteemed institutions.

I would like to express my sincere gratitude to my primary supervisor Dr. Norman Kerle for his tireless support, lessons and guidance in carrying out this study. I am also very thankful to him for continuous encouragement he gave me to improve my work and the patience he showed for all ups and down during the study. His guidance helped me to gain lot of scientific experience. I am very much grateful to my second supervisor Dr. Menno Straatsma for providing me all the data and materials for this research. I am also thankful to him for his contribution in this research.

My special thanks to Dr. Sokhon Phem, lecturer, ITC, for his invaluable support and guidance during the initial stage of the research.

I would also like to thank Prof. Ted Milton, Prof. Petter Pilesjo, Prof Andrew Skidmore, Prof. Katarzyna Dobrowska, Dr. Andre Kooiman, Ms. Steff Webb and Ms. Jorein Terlouw for their support and hospitality during the entire course of my study. I am also thankful to all the teachers of the consortium institutes for enriching my knowledge through their lessons.

I gratefully acknowledge my parents for their endless moral support and encouragement during the entire course of study. My special thanks to Niladri for always being with me and supporting and encouraging me in every step of my life.

Finally, I would like to thank all my friends and classmates from around the world for sharing their friendship and knowledge during the course of study. Because of them I enjoyed every bit of the journey in the last one and half years.

Table of contents

List of Figures

List of Tables

Abbreviations

AHN	Actueel Hoogtebestand Nederland
ASTER	Advanced Space borne Thermal Emission and Reflection Radiometer
CRED	Centre for Research on Epidemiology of Disasters
DEM	Digital Elevation Model
DSM	Digital Surface Model
DTM	Digital Terrain Model
GCP	Ground Control Point
GIS	Geographical Information System
GLCM	Gray Level Co-occurrence Matrix
GPS	Global Positioning System
IDW	Inverse Distance Weighting
IPCC	Intergovernmental Panel on Climate Change
LiDAR	Light Detection and Ranging
NDVI	Normalized Difference Vegetation Index
RMSE	Root Mean Square Error
SD	Standard deviation
SPOT	System Pour l'Observation de la Terre
TIN	Triangulated Irregular Network
UNESCO	United Nations Educational, Scientific and Cultural Organization
USGS	United States Geological Survey
UTM	Universal Transverse Mercator
WGS	World Geodetic System

1. Introduction

1.1. Natural Hazards

Natural hazards are natural events in the physical environment occurring with unusual magnitude and scale and threaten the life and property of human being as well as the environment. According to UNSECO (2008) "Natural hazards are naturally-occurring physical phenomena caused either by rapid or slow onset of events having atmospheric, geologic and hydrologic origins on solar, global, regional, national and local scales " and “natural disasters are the consequences or effects of natural hazards, but natural phenomena do not automatically have to spell disaster.” The occurrences of natural disasters are on the rise. According to Munich Reinsurance (2007) the number of natural disasters are increasing over the last three decades and the number of catastrophes recorded in 2007 (950) has been found to be the highest since 1974. The trend indicates more extreme events in the future.

More than 18% of these natural disasters are occurring in developing and emerging countries. Among the 50 most significant natural catastrophes in 2007 throughout the world 42% occurred in developing countries accounting for enormous economic and social losses. Flood and storm accounted for around 40% of the overall losses due to natural hazards in the year 2007 (MunichReinsurance, 2007).

1.1.1. Flood Scenario

The number of flood events has increased in many parts of the globe in last two decades (Appendix A1). A report by Centre for Research on Epidemiology of Disasters (CRED, 2005) showed that the total number of flood events in the world has increased from 107 in 2004 to 168 in 2005.

Flood has been defined in different ways depending on its nature and location. According to the definition of U.S. Geological Survey (USGS) “a flood is an overflow or inundation that comes from a river or other body of water and causes and threatens damage” (http://ks.water.usgs.gov). Flood can be broadly distinguished into two types namely river and coastal flooding. River flooding is caused due to excessive run off and overflowing of river and the coastal flooding is the result of storm surges. The majority of the flood events are the result of direct and indirect climatological reasons. Climate change and deforestation also potentially contribute to the problem (IPCC, 2007). Glacial lake outburst, dam failure, river straightening and surface sealing are important among the other causes of flood. The severity and impact of flood depends on the nature of terrain (e.g. slope, aspect, soil type and vegetation cover), the channel characteristics (e.g. depth, length and roughness) and the landuse of the surrounding area (Green *et al.*, 2000).

Apart from the natural and structural causes there are some social causes which enhance the impact of floods. Rapid urbanization and increasing population are driving people to encroach to the marginalised land in the floodplain area and thus increasing their vulnerability due to flood events. Moreover, the lack of efficient early warning system and disaster preparedness results in losses of life and property, especially in developing countries. Thus, we should be concerned about the flood hazards, not only for its severity and impact but also for its number and frequency of occurrence.

1.1.2. Geoinformation for flood hazards

Keeping in mind the increasing trend of flood events in many parts of the globe, efficient disaster risk management is necessary. The process of disaster risk management can be divided into two distinct parts namely pre and post disaster risk management. In both the processes geoinformation is an efficient tool. It is a multi-disciplinary information system which combines all the relevant attributes for flood hazard from different sources, analyse them and represents a decision making system for disaster management. Remote sensing, GIS and GPS are the integral parts of the geoinformation system. It uses the spatial information from remote sensing sources, location information from GPS and combines them with aspatial information in a GIS platform to generate user compatible information. Several studies have been successfully carried out for flood management using geoinformation technique (Rango and Anderson, 1974, Sanyal and Lu, 2004, Brivio *et al.*, 2002, Bates *et al.*, 1997, Profeti and Macintosh, 1997, Portmann, 1997).

1.1.3. Flood models: data requirement and sources

Flood models are integral part of flood risk management. Every flood model needs to be parameterized before simulation. Three basic components of a flood model are: 1) detailed information about the surface topography which is broadly termed as digital elevation model (DEM), 2) surface roughness and 3) inflow hydrograph (van der Sande *et al.*, 2003). The terrain height is the fundamental requirement for flood models because it determines the flow pattern and resultant flooded area in the floodplain to a large extent. Remote sensing is widely used to map the terrain height by deriving DEMs. However, automatically derived elevation models from remote sensing data represent both the ground surface and the objects lying on the surface at scale of resolution of the image (Kasser and Egels, 2002). This is also true for photogrammetrically derived surface models which are the oldest and still most frequently used method for DEM generation. The resulting type of representation is termed as Digital Surface Model (DSM). DSMs are very important because it is possible to identify the terrain features on the DSMs and obtain the ground elevation which is an essential element for flood modelling. The model which is developed by eliminating the surface features from DSMs is termed as Digital Terrain Model (DTM) (Figure 1-1). Thus a DTM is a derivative of DSM and it is a true representation of bare earth surface. In an open area without any landcover feature, DSM is identical to DTM (Priestnall *et al.*, 2000).

DSMs are widely used in studies on surface features e.g. vegetations. It has application in canopy modelling and biomass estimation (NÃsset, 2002, Koukoulas and Blackburn, 2005, St-Onge *et al.*, 2008) However, for flood modelling it is necessary to know the surface topography without the artifacts which are not relevant for flood modelling. Some of the artifacts pose obstruction to water flow and some do not. A model with non-obstacles does not provide the accurate information about different components of water flow. Thus, the most critical issue is the identification of relevant and important non-obstacles in a DSM to generate a DTM that will be used for flood models. This conversion process is most crucial because errors in DTM affect the determination of flow path, flow accumulation, and different surface derivatives like slope and aspect and thus produce errors in discharge hydrograph (Oksanen and Sarjakoski, 2005, Veregin, 1997, Wise, 2007). The potential effects of these errors in risk assessment and flood management highlight the importance of optimizing the topographic data quality.

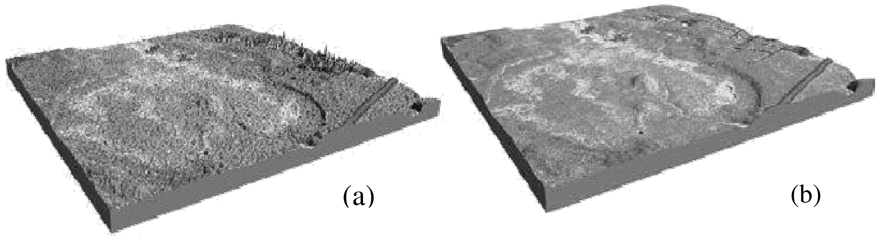

Figure 1-1 (a) Digital surface model and (b) Digital terrain model (Source: http://pubs.usgs.gov)

Topographic information can be obtained either by detailed topographic survey or using remote sensing methods such as photogrammetry, laser and microwave techniques. Using properly oriented pairs of stereoscopic photos of same scale, surface height can be obtained photogrammetrically by measuring parallax. Remote sensing satellites such as ASTER, SPOT, IKONOS and QuickBird produce stereo images. Stereo images are also available from airborne remote sensing platforms. In addition to this, GPS measurements can be used to assess the accuracy of photogrammetrically derived surface models.

Among all other techniques of creating DTMs, photogrammetry is the oldest technique, with developments already beginning around 1840 (Falkner, 1995). The principle of photogrammetry was known since the invention of photography and simple pinhole camera. Aerial photography from a plane started during 1903, which was a milestone in the field of aerial photography. It has been extensively used in defence purposes. Several government departments and federal agencies (e.g. U.S Geological Survey and British Ordnance Survey) have rich archive of old aerial photos (Itaya *et al.*, 2004). Digital photogrammetry started during the decade of 1970s (Mikhail *et al.*, 2001, Falkner, 1995). During the last few decades digital photogrammetry has improved significantly and with the new techniques photogrammetry will flourish more in future. The feature extraction from images is no more burden using different semi-automated and automated techniques of photogrammetry. In the context of this research high resolution aerial photos are potential source to derive DSMs and DTMs. Therefore, it is necessary to explore how photogrammetrically derived DSMs from aerial photos can be improved and made suitable to use in flood modelling.

1.2. Problem Statement

As mentioned earlier DTM is the most important component of flood models and it is generated from DSM by removing the artifacts. However, it is essential to understand which of the artifacts should be removed and which can be kept in the DTM for using it in a flood model. Features obstructing the water flow should not be removed because they influence the flow rate and flow path. The other features may be removed if they are not resisting water flow because in such areas the ground characteristics control different components of water flow. In some studies DSM has been used as the ground information for flood analysis (van der Sande *et al.*, 2003, Peters *et al.*, 2006) and in some other studies DTM has been used instead of DSM (Choi *et al.*, 2008, Wu *et al.*, 2008, Mason *et al.*, 2007, Forte *et al.*, 2006). Considering different studies, what is the most suitable surface model to be used in flood modelling is not well understood. It may be more logical to use a pseudo-DTM (Figure 1-2C) by removing the irrelevant artifacts from a DSM, instead of using a pure DSM (Figure 1-2A) or a pure DTM (Figure 1-2B). This aspect has not been well explored. Therefore, it is necessary to identify what kind of surface model is the most suitable for flood models.

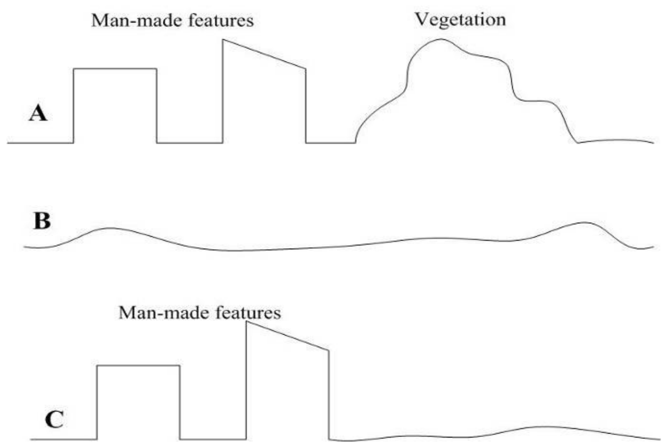

Figure 1-2 Pictorial representation of (A) a DSM, (B) a DTM and (C) a pseudo-DTM.

After that the most obvious question is how to remove the irrelevant artifacts from a DSM? Many studies have been done on removing artifacts from DSMs. All the present methods incur some error and the error increases as the terrain slope increases. It is because in the areas with a certain slope simple interpolation of known height over the whole area will not work well as it does in flat areas. Thus, DTM derived using those approaches in highly elevated area will lead to wrong estimation in flood model. Moreover, error generates in different stages of DTM generation starting from the image acquisition process. Apart form that, in areas with complex and heterogeneous landcover, the process of identification and removal become complex and thus induce errors. It is still a challenge to remove all the sources of error. Therefore, there is a need to develop a method that can remove the artifacts from the DSM with minimum error.

In this regard, it is necessary to identify the relevant artifacts that should be removed from the DSM, measure their heights in the DSM and develop a method to remove them to derive a DTM suitable for using in flood models. It is also necessary to quantify the errors involved in this process.

So far ample work has been done in creating DTM from laser and radar techniques due to their high precision in image acquisition, but the data are not available for all parts of the world. Aerial photos being widely available and inexpensive and photogrammetry being the oldest technique in surface model generation; they can potentially be used for generating DTMs for flood modelling.

1.3. Research Objectives and Questions

The main objective of this research is to develop a suitable semi-automatic method to identify relevant artifacts (which do not pose obstruction to water flow) on the DSM and remove them from the DSM to generate a pseudo-DTM for using it in flood analysis. The study also aims to find out the sources of errors involved in the development of DTM, measure them both qualitatively and quantitatively. The study intends to assess and estimate the errors in the pseudo-DTM by comparing it with the DSM and with an existing DTM derived from LiDAR data.

The specific objectives and related research questions of this study are as follows:

Specific objectives	Research questions
1. To find out relevant artifacts in the DSM that should be removed from the DSM to develop a DTM for flood modelling using photogrammetry.	1. What are the relevant artifacts that should be eliminated from the DSM to generate DTM for flood modelling?
2. To develop a semi-automatic method to remove the relevant artifacts from a DSM to generate a pseudo-DTM suitable for flood model.	2. Is it possible to formulate a semi-automatic method to develop a pseudo-DTM suitable for flood model by removing relevant artifacts from the photogrammetrically derived DSM?
3. To assess the horizontal and vertical accuracies of the pseudo-DTM with respect to the DSM and the reference LiDAR DTM.	3. How good is the pseudo-DTM compared to the DSM? What are the accuracies of the derived DTM with respect to the reference LiDAR DTM?

1.4. Hypothesis

The research will be carried out considering the following hypothesis:

Ho: It is not possible to identify and remove the impermeable obstacles to water flow effectively from a photogrammetrically derived DSM using semiautomatic method.

H1: It is possible to identify and remove the impermeable obstacles to water flow effectively from a photogrammetrically derived DSM using semi-automatic method.

1.5. Research Approach

The research will be carried out in the following phases.

1. The first phase of the research has covered the introduction and relevance of the topic, the problem identification and the objective and research questions of this study (Chapter 1). It will also include review of existing literatures related to the topic. It will provide detail understanding of flood model requirements, surface models used in different studies, different methods to generate the surface models and errors involved in them and the methods to reduce the errors. Through gap analysis this chapter will clarify the objectives and research questions (Chapter 2).

2. The second phase will focus on the study area and data available for this study. It will also include aspects of pre-processing of the available data (Chapter 3).

3. The main research work on data analysis and method development will be described in this phase (Chapter 4). It will consist of the detailed explanation of the results obtained from the study and the discussion about the results (Chapter 5 & 6).

4. The final phase (Chapter 7) will conclude the above research with a focus on the future perspective of the study.

2. Literature Review

2.1. Introduction

As schematized in the research approach this chapter will provide a brief overview of the flood models, their requirements and importance in flood analysis. This chapter will also emphasis on the different methods which are used to extract information about the surface features such as their characteristics and height. Different errors in deriving elevation model, their impacts on the flood model output and the methods to minimise those errors will also be addressed in this chapter. Lastly this chapter will focus on some critical issues and problems in deriving the elevation model.

2.2. Flood models overview

A model is a representation designed to depict an object or a system or a concept of the real world and it delivers simplified explanation of complex systems. Similarly, a *hydrological model* is an approximation of an actual hydrological system. The measurable hydrological variables are the parameters of a hydrological model and the structure of the model is comprised of some equations representing interrelationship among the corresponding variables.

Flood inundation is modelled using *hydrodynamic or hydraulic models*. They apply the principle of conservation of mass, momentum and energy and quantify the flow of water as a function of surface topography (Alkema, 2007). Hydraulic models range form simple one dimensional to more complex two dimensional. In 1D hydraulic model the water flow is estimated in one dimension. In this case the water velocity and its depth are measured as a function of time and space in the longitudinal direction. HEC-RAS, MIKE-SHE and LISFLOOD-FP are some examples of 1D hydraulic model. On the other hand, 2D hydraulic models analyse the water flow in both X and Y directions on a horizontal surface. Free surface flow can be described using these models. These models are especially important in the areas which are heterogeneous in terms of landcover and the flow is affected by those factors in addition to the elevation of the area and the channel. 1D model can be used in channel or stream flow with the artifacts such as culverts and bridges, whereas the 2D models can be used for floodplains with complex landcover including buildings and roads. SOBEK, MIKE 2, TELEMAC-2D 1 and FLO-2D are some examples of 2D hydraulic models (Horritt and Bates, 2002).

2.2.1. Flood model requirements

All flood models (1D and 2D) need some spatial and non-spatial attributes as the basic input (Table 2-1).

Table 2-1 Basic inputs of a flood model

Spatial information	Non-spatial information
Surface roughness	Inflow hydrograph (initial water level).
Digital elevation model	Boundary conditions

The *surface roughness* is described as the resistance to the flow of water. It mainly depends on the type of land cover in the floodplain area and type of bed material in the channel. It is generally expressed as Manning's roughness coefficient (Chow *et al.*, 1988, Alkema, 2007).

Digital elevation model (DEM), in general, is a model which provides digital and mathematical representation of objects and its environment on the earth's surface. It provides information in X, Y and Z directions and consequently the terrain height information. However, this representation is different according to the purpose of its use. DEM is a generic concept which may refer to the elevation of ground but also include all objects above ground such as buildings, roads and vegetation (Kasser and Egels, 2002). On the contrary, according to Maune (2001), DEM represents the elevation of the earth's surface devoid of the surface features unless it is referenced as a DSM. Therefore, to remove the confusion, the DEM is termed as DTM when the information is limited to the bare earth's surface whereas it is termed as DSM when it includes the surface features. Specifically, for flood modelling purpose, the elevation model should contain those surface features that affect the flow of water. In that case, the model is neither a true DSM nor a true DTM. This model may be termed as pseudo-DTM.

The *inflow hydrograph* refers to the initial condition of the hydrological system (water level and flux). *Upstream and down stream boundary conditions* are defined as the amount of water entering in to the system in the upstream area and leaving the system in the downstream area (Alkema, 2007, Chow, 1964).

2.2.2. Surface models and their importance in flood modelling

As mentioned in the previous section, the surface model needed for the flood modelling purpose can be a pseudo-DTM which should contain the features affecting the flow of water while the other features can be omitted. Accordingly it is necessary to understand which features actually pose obstruction on the flow of water during flood and should be reflected in the surface model to analyze flood events.

Natural and artificial obstacles considerably affect the flow of water. In a heterogeneous landscape the man made structures such as buildings, industrial and commercial structures, dikes, bridges and dams generally act as impermeable obstacles for water flow whereas water passes through the roads, canals, sewer systems, meadows, open areas and through vegetated areas. However, the nature of obstruction also depends on the scale and intensity of the flood event. If the intensity of a flood incident is high enough, the buildings and dams can be crushed by the high velocity water flow. Moreover, in high intensity floods majority of the flow passes through the streets, canal and sewer systems. In those situations the obstacles such as buildings and industrial and commercial structures will act as permeable obstacles to water flow. On the other hand, these objects will act as impermeable obstacles to water flow in medium and low intensity flood events (Mignot *et al.*, 2005, Frazão *et al.*, 2004). In such cases even features such as culverts play an important role in changing flow directions (Maidment, 1993). Thus while using a surface model for flood modelling the obstacles should be considered at the scale of the flood intensity.

In fact, studies on flood are often carried out overlooking these topographical details. In flood prediction studies using models, the topographic information is very important because very small changes in the topography (±10 cm) can significantly affect the model prediction. This is particularly true for the 2D flood models which describes the spatial distribution of flow rather than the bulk flow (Marks and Bates, 2000). DEMs are widely used in flood models and flood hazard analysis as the topographic information. However, in many cases it is not even mentioned if the surface model actually is a DSM or a DTM (Sanyal and Lu, 2004). In some studies the importance of objects posing an obstacle have been overlooked (Forte *et al.*, 2006) while in other studies DEM are mentioned as the surface model for flood mapping without any clarification if it a DSM or a DTM (Peters *et al.*, 2006). Marks and Bates (2000) has used a LiDAR derived vegetation corrected DEM to simulate a flood model but did not mentioned the need for retaining the surface features which may act as obstacle to water flow. A "bare-earth" DEM was also used in a study of flood related inundation vulnerability in Victoria, Australia (Wheeler *et al.*, 2007). In different raster based DEMs available globally the linear topographic features such as dams and ridges are not represented due to their coarse resolution. Portmann (1997), in a study on runoff modelling using remote sensing data on the river Rhine, mentioned the need of incorporating the relevant topographic features (e.g. culverts) in the raster DEM to obtain a pseudo-DTM. Some studies do stress on the fact that relevant surface features such as buildings should be retained in the DTM that is to be used for flood modelling purpose. Mason (2007) used a pseudo-DTM (with man made structures and without vegetation) for urban flood modelling, and particularly stressed the need to remove the flyovers and bridges from the DTM because they act as artificial blockage to the flow of water.

Thus, while deriving a suitable surface model for flood risk management purpose, the first and foremost requirement is to decide on the obstacle and non-obstacle ground features at a specific scale of a flood event. This explains the scope of the first objective of this study (section 1.3).

2.2.3. Digital model representation

The principal component of flood model is the information about surface topography. They can be derived from different sources using different methods. The following sections will provide a brief overview of those aspects in the context of photogrammetry.

The topographic surface mathematically is a continuous surface. Irrespective of the source image, the main principle of deriving a topographical surface is to select sample points representing the topographical heights and then to interpolate them to construct a DSM. There are three common forms of representation of elevation models which are (1) regular raster grid, (2) triangulated irregular network (TIN) and (3) contour or iso-line based models.

In *regular gridded DSM* the terrain is represented as the elevations sampled in regular array of square grids. Each cell represents an area of earth at a definite unit and it has a height value. In *triangulated irregular network (TIN)* the terrain is represented as the elevation sampled irregularly over an area and connected together to form a series of triangles covering the area. The triangles are generated by the Delaunay Triangulation method (Longley, 2005). *Contour based model* can either be generated from the historical topographical sheets or from stereo pairs. The toposheets are scanned and digitised to generate equipotential lines. From the stereo pairs the contour lines are generated automatically using suitable software (Hutchinson and Gallant, 2000). The contour lines can also be developed from stereo pairs with an underlying surface model such as TIN and grid representation..

2.3. Methods to convert DSM to DTM

In fact it is necessary to know the elevation values of different points in the image prior to interpolation to represent the DSM either in grid or TIN or contour based format. In automatic photogrammetric method this height information is generated during stereo-matching by quantifying the parallax between the stereo pairs. All automatic techniques generate a DSM unless and until they are corrected for objects manually or semi-automatically. As the DSM contains all the surface features, the elevation model will describe the rooftop and canopy structure along with ground elevation in areas with heterogeneous landcover. For generating a DTM the raised structures such as vegetation and buildings should be removed and for flood modelling purpose only the relevant features should be removed. Then the surface should be interpolated through the blank spaces created after removal of the objects. This analysis can be done using different ways such as traditional image classification, object oriented classification, filtering techniques and using different algorithms.

2.3.1. Image Classification

The DSM developed from stereo pairs provides the height information of ground as well as non-ground objects. This information is available for each pixel of the corresponding image. The artifacts can be identified from a cluster of raised pixel from the ground height. The method of identification of different features in scanned aerial photograph is different from that of multispectral images. The main characteristics of the features which are used to segregate them in that data are shape, size, pattern, tone, texture, shadow, site and association.

In many cases ***image classification*** techniques have been used to recognise the surface features for example buildings as building and trees as trees (James *et al.*, 2006, Zebedin *et al.*, 2006, Baillard *et al.*, 1998, Knudsen, 2005). However, simple classification based on spectral separation is sometimes combined with information about the texture. Colour and spatial relationship of the features in the image are considered to improve the classification quality. The major problem in classification arises during overlapping signature of landcover classes. Ancillary information such as texture can improve the classification efficiency.

Texture provides a visual perception of coarseness and smoothness of images and thus can segregate different features in the image. Texture can be estimated using different approaches such as structural approach, model based approach (e.g. Markov random fields and auto regressive model) and feature based approach (Coburn and Roberts, 2004). Among them the most successful and widely implemented method is the feature based texture analysis and classification method. It involves the analysis of spatial information and the statistical attributes of the image. First and second order texture descriptors are used in this regard. The first order descriptors involve statistical properties such as mean, median, standard deviation and variance of texture of a cluster of pixels, whereas the second order statistics measure the mutual dependence of a set of pixels and characterise their distribution over a space. The most popular second order statistical method for texture analysis is Gray Level Co-occurrence Matrix (GLCM). GLCM is a probability matrix which measures the relationship of the pixels neighbourhood on the basis of their gray level values (Appendix B1). The examples of the second order texture measures in GLCM are homogeneity, angular momentum, contrast, entropy and dissimilarity (Coburn and Roberts, 2004, Ge *et al.*, 2006, Jensen, 1996). Different studies were carried out using texture measures. Hudak and Wessman (1998) used texture of different plant species as an index to recognise plant species and found that texture is a good indicator of woody plants, though it may not be proved to be good for other canopies. Texture analysis using GLCM was used by Ge *et al.* (2006) to map an invasive plant species in California and the classification results show the producer's and user's accuracies as 77.89% and 71.33% respectively. Caridade *et al.* (2008) used eight different texture measures to classify landcover in a national park of Peneda-Gereˆs in northwest Portugal using black and white aerial photo. In about 80% cases trees and shrubs and in above 85% grassland were correctly classified. Different window sizes were also used in their study which showed that the grasslands were most efficiently classified using 3 X 3 window whereas 7 X 7 window was most efficient for classifying trees and shrubs. Several other studies by Gong *et al.* (1992), Ryherd and Woodcock (1996), Sali and Wolfson (1992), Wudler *et al.* (1998), Mohamed and Kim (2003), Lovan *et al.* (2007), Zhang *et al.* (2003) and Garcia and Puig (2007) found texture as an efficient measure to improve the classification accuracy especially using aerial photo where spectral information is not available.

Decision rule based classification such as ***fuzzy classification*** is now being used for feature identification. This approach performs well when one pixel is described by more than one class and also in transitional zone of different landcover classes (James *et al.*, 2006, Samadzadegan *et al.*, 2005). The detection of landcover features can also be done by shape recognition using ***segmentation*** techniques. The extension of the surface features can be detected by segmentation and then DTM can be generated by interpolating known ground elevation values. This segmentation can either be done using only a DSM or by using an orthophoto along with the DSM to improve the reliability of the process (Kasser and Egels, 2002). Waser *et al.* (2006) reported a two-stage multi-resolution segmentation and fuzzy classification method of orthophotos to identify vegetation classes in Eigenried, Switzerland. Segmentation followed by context-based data analysis was successfully done in identification of road network in urban environment using DSM from aerial photo except in some complex environment (Hinz and Baumgartner, 2003).

2.3.2. Algorithms and filters

Different ***algorithms*** have been used for automatic detection of surface features, especially buildings (e.g. shadow analysis based algorithm, fusion based system and wavelet algorithm). The development of different algorithm is
described by different authors (Lu *et al.*, 2006). All the algorithms are specific for particular application and are not necessarily transferrable to any other environment. Lu *et al.* (2006) described a method of building identification using aerial photo and high resolution multi-spectral data. The authors used a rigorous method using landcover classification, k-mean clustering and NDVI based classification and fused those results with the DSM using Dempster-Shafer data fusion theory to detect the actual building position and shape in the image. Another way of identifying and removing surface objects is ***filtering***. This technique assumes that the raised structures constitute a connex zone and it has high contrast in elevation with respect to the surrounding (Kasser and Egels, 2002). Mathematical morphology is the basis of this method. Different filtering techniques were widely used in DTM generation especially using LiDAR data (Liu, 2008, Marks and Bates, 2000). These techniques perform well in plane land but fails in hilly areas and areas with vertical slope and sharp ridges. Sithole and Vosselman (2003) compared eight different filtering algorithms and concluded that in areas with sharp surface discontinuities these methods struggle. James *et al.* (2006) described the filtering methods as "unintelligent" to differentiate the ground and the surface features.

The majority of the studies reviewed above required some ancillary information or supporting data such as LiDAR and satellite images. There is a need of developing a suitable method of creating a DTM from a DSM by eliminating the relevant surface features using aerial photos or other high resolution data only, without the input of additional data. Thus the motivation for the second objective of this study (section 1.3) is clarified.

2.4. Sources of errors in DSMs and DTMs and effects on flood model

It is well understood that the topographic information is the most important parameter in flood modelling and that errors in it can introduce errors in the result from models. The errors in original surface propagate through different stages of the model and produce compounded effect in the final result. In hydrological studies different derivatives of DEMs, such as slope and aspect are used and they are highly sensitive to the errors in the original surface. Errors in DEM can occur in both vertical and horizontal direction, though the importance is more for the vertical errors because they represent the errors in elevation. The errors may be defined as the mistake that can be avoided if enough care is taken. However in case of spatial data and analysis often the errors can not be avoided. Thus the sources of errors should be understood and should be accounted for.

The errors in elevation model can be introduced in two major stages of DEM generation namely during the image acquisition stage and pre-processing stage, as well as during image processing stage. These errors can be categorised as *data based errors*, *model based errors* and errors based on the *characteristic of the terrain* which is being sampled and modelled (Fisher and Nicholas, 2006).

2.4.1. Data-based errors

The data based errors are generated during the image acquisition and pre-processing stage. In this stage the errors generate due to several reasons such as errors in camera and flight parameter calibration, accuracy, density and distribution of source data, photo scanning parameters and poor image quality. Historically, DEMs were generated by digitising contours from aerial photography or point measurements from land survey. One of the major disadvantages of interpolation from contour is that they over estimate the elevation at certain heights and can not produce elevation information between those heights. Thus contour based DEMs are often found to be suffered by systematic errors (Wise, 2000, Kerle, 2002). Wise (2000) very distinctively described the error in DEM from contour due to variation of model. The author described the lattice model (considers the height of the centre of the pixel) to be more appropriate than pixel model which is basically an area based model. In the later case if the contour does not pass through the centre of the pixel interpolation errors generate which then propagate through the model. Later on traditional hard copy aerial photographs were scanned to obtain the digital format. The scanning resolution governs the size of the pixel in digital format and thus the amount of information in each pixel. The higher the resolution easier will be the identification of features in the image. Smith *et al.* (1997) have shown the effect of scanning resolution on the resulting DEM accuracy from aerial photographs (Appendix B2). Interpolation also induces potential errors in contour based DEMs. Manual and semi-automated photogrammetric methods are often associated with random and systematic errors; for example errors due to failure in identification of precise target point during aerial triangulation process and instrumental errors respectively. Image quality and the radiometric properties of the pixels influence the image matching algorithm. The density of DEM posts also influences the accuracy of the DEM.

2.4.2. Model-based errors

Model based errors are generated during the second stage of DEM generation i.e. in the processing stage. This stage involves processing and the interpolation of measured data to derive a DEM. The data acquired through remote sensing do not contain the height information at all the points of the sampled area. Therefore, to obtain continuous height surface the information are needed to be interpolated throughout the surface. The degree of interpolation depends on the distribution and density of the source data and this itself is a source of error. The interpolation can be done either using a direct modelling in the form of TIN or using indirect modelling by random to grid interpolation. A variety of methods are available for the indirect modelling such as inverse distance weighted (IDW) interpolation, thiessen polygon, spline and geostatistical kriging (Appendix B3). Among them the geostatistical kriging is an attractive option for interpolation from a statistical standpoint and this method also generates linear unbiased estimations, but the variance is found to be directly proportional to the distance of the interpolated value from the input observation (Longley, 2005, Burrough and McDonnell, 1998). No single interpolation method is perfect. Furthermore, the accuracy of interpolation depends on the nature of terrain surface and distribution of sample points (Fisher and Nicholas, 2006). A great variety of research has been done on the method of interpolation and the error in DEM and none of the methods has been found to be appropriate for all types of terrain. Gong *et al.* (2000) found that the accuracy of DEMs in terms of RMSE increases as the terrain slope increases (Appendix B4). Similarly, Rees (2000) reported the RMSE of interpolated DEM to be directly proportional to the standard deviation of the height difference between adjacent points in DEM.

The majority of the hydrological models use gridded DEMs as the source of terrain information because of the mathematical simplicity. One major problem in gridded DEMs is that they underestimate the terrain in rugged area and oversamples in smooth areas (Wise, 2007). Thus the resolution of the grid cells is an important factor. High resolution grid cell can depict the surface in more detail than the coarse resolution cells do. During interpolation the sub-grid information are often suppressed especially in DEMs with coarse grid cell resolution. Hydrological derivatives such as flow direction, channel network and flow extracted from DEM are directly influenced by the grid resolution (Wechsler, 2007).

2.4.3. Errors based on the terrain characteristics

In continuation of the above section it can be said that the terrain characteristics can directly influence the accuracy of a DEM. In general, the accuracy of DEMs decrease with increase in the relief and the complexity of the terrain (Gong, 2000, Carlisle, 2005). Moreover an area under consideration can be a combination of water, vegetation, flat area, steep terrain and other man made objects. The accuracy of a single DEM in such an area can vary depending on the landcover and the terrain characteristics (Appendix B5). The DEM from stereo aerial photography has been found to have more errors in the steep, shaded and vegetated areas than in the flat terrain. Linear interpolation will not be appropriate in steep areas because in such areas with significant breaks of slopes the terrain shape is lost during interpolation. In vegetated areas the ground height information are not recorded in remote sensing sources such as aerial photographs. Thus sudden change in relief or terrain character will be undersampled in those areas. In automated digital photogrammetry the micro relief of terrain and local slope are often overlooked which reduces the accuracy of the elevation model.

DEMs often contain sudden height variations which are termed sinks or pits. They are generated when a cell is surrounded by cells with higher elevation. To estimate the hydrological parameters such as flow accumulation and flow direction these sinks should be removed. However, the sinks are treated as artifacts in DEMs and often eliminated by sink filling. Sometimes the sinks can be real where surface hummocks and hollows are present. Thus without investigating the presence of sinks in reality, sink filling can incorporate errors in DEMs. It was found that the sinks are more frequent in flat terrain than in the hilly terrain (Wechsler, 2007). Kerle (2002) reported the sensitivity of the matching algorithm to terrain and evidences of spikes and ridges of about 150m which were obtained typically from area based image matching. From the above discussion the motivation for the third objective (section 1.3) is clarified.

2.4.4. Methods to reduce errors

For the reduction of the data based errors the use of high resolution data is often recommended. The higher the resolution the higher will be the precision of all measurements. In this regard LiDAR data has been used by several studies because of its capability of generating high density elevation data (Smith *et al.*, 1997, Fisher and Nicholas, 2006). To minimise the errors of interpolation high resolution grid is suitable. It can minimise the generalisation of terrain characteristics but still is not possible for sub-grid level generalisation without substantial ground verification or without the use of high density point data such as LiDAR. In the steep slope area local slope can be taken into account while making error correction. For example, as James *et al.* (2006) pointed out in their study, a mean elevation can be taken into account instead of minimum elevation while performing filtering to minimise the underestimation of the terrain. Sinks in the DEMs are considered as artifacts and they are usually removed from the model. Sinks can be identified by examining the impediments to a flow in the DEM. The general methods which are used to remove the sinks are sink-filling and breaching or a combination of both. Sink filling raises the elevation in the locations which are undersampled and breaching lowers the elevation in the locations which are oversampled. However, before undertaking these methods it is necessary to know if the sink is real or an artifact. Wechsler (2007) pointed out the method of identifying sinks as very time intensive. It includes extensive ground verification, examination of the source data and developing a classification model for a particular DEM and using it to identify the depressions in the DEM. Lindsay and Creed (2005) mentioned knowledge based approach to identify the artifacts.

2.5. Height estimation from aerial photo

Aerial photography are the oldest remote sensing technique being in use since 1840 (Falkner, 1995). One of the major reasons for this technique being very popular and extensively used is their capability of generating height information of the landcover features from the parallax along with the spatial information. This height can easily be perceived by viewing a stereo model in appropriate interface. In the context of flood modelling these key properties of features can be used to identify the features in the aerial photo and remove them from the DSM. Knowing the height of object and the ground height above mean sea level, the later can be subtracted from the former to obtain the DTM. The subtraction of height can either be done using the in-built algorithm in different software or manually or interactively by pixel wise editing.

The estimation of the height of features has been in concern from long time. A number of possible techniques used earlier (during 70's) have been summarised by Tuner and Steiner (1979). Ground measurement of height of features is still being used as the most reliable method of height measurement. Conventional photogrammetry is also used for this purpose though it is a time consuming and expensive process. The use of stereo orthophotograph is also useful equipment both for the feature recognition as well as height measurement. Baltsavias (1996) reported it to produce more accurate height measurements than an elevation model. Shadow analysis is another method which was used to determine the object height, where the height of the shadow represents the height of features. The contrast analysis was carried out by Massalabi (2004) to identify the potential shadow zones and segmentation followed by classification was used to finally detect the shadows. Knowing the sun elevation, the sun azimuth, the relative position of the sun, shadow and the sensor from the metadata of the images it is possible to calculate the height of objects. An altimetric segmentation of DSM followed by region growing algorithm was proposed by different authors to identify the ground and non-ground objects and measure their height. Binary classification of the segmented images were also performed to obtain the DTM (Baillard *et al.*, 1998, Cord *et al.*, 1999).

2.6. Some critical issues

Determination of the appropriate resolution of a DEM needs an understanding of both the fidelity of the surface as well as the practicality of handling source data and derived product. High resolution DEM always facilitates a better understanding of the area under consideration by depicting detailed surface representation. However, the requirement of the resolution of DEM and the required amount of detail in DEM depend on the application of the derived DEM. In areas with moderate and low topographic variability the coarse resolution DEMs are preferred. On the other hand, in areas with complex topography such as sudden variation in height, high resolution DEM is often preferred. However, in coarse resolution DEM the information (especially sub-grid information) are often generalised. This generalisation of topographic characteristics also affects different surface derivatives and different component of flood models. The flow routing, channel network, flow accumulation and discharge are affected due to change in topographic nature. The effect of resolution of DEMs on hydrological analysis was well summarised by Wechsler (2007) and Kenward *et al.* (2000) and also mentioned in the section 2.4. In spite of the factors mentioned above in support of the high resolution DEMs one question which always pops up is that is it always useful or favourable to use very high resolution DEMs for flood modelling? The answer is probably not. The high resolution DEMs are necessarily not better than coarse when computation time for analysing the DEM is considered. High resolution data slows down the computation process of different derivatives and also potentially contributes to the error propagation in deriving them. Thus, the choice of grid resolution depends on the topographic complexity, nature of analysis, resolution of the source data and of course on the practical considerations such as finance and time.

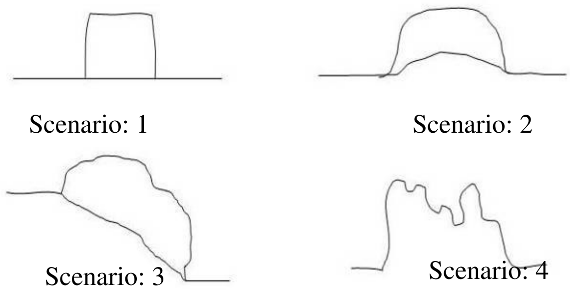

Figure 2-1 Different scenario in deriving DTM for flood model

Another potential point of concern is the surface interpolation in variable terrain condition and in areas with intra-class variation in different landcover features. In the most simple case as in scenario 1 (Figure 2-1) it is possible to obtain the ground height and the height of the landcover feature, which can then be subtracted from the ground height and the surface can be interpolated to obtain the terrain. However, in cases as depicted in scenario 2, 3 and 4 this approach will lead to incorrect estimation of the terrain. If there is any feature that bulges out under for example vegetation that may act as obstacle to water flow and it is necessary to characterise the feature in the DTM. Simple subtraction of the height of the vegetation and interpolation of the ground height would underestimate the terrain and would not produce the correct surface. Areas with intra-class height variation (scenario 3 and 4) require special attention during interpolation because all the wrong estimations ultimately result in incorrect estimation of terrain and surface derivatives and accordingly influence the discharge hydrograph in flood model. These problems are still being a challenge in proper understanding a terrain, and therefore, require more attention to produce a surface model with better accuracy.

2.7. Summary

Based on the studies mentioned above, it can be said that not very much attention has been given in the uncertainty in the elevation model due presence of different landcover features, which is very important in flood modelling. In most of the studies on developing elevation model using aerial photos the height accuracy has been improved with the help of either extensive ground verification or using high density data such as LiDAR. Photogrammetry being an inexpensive and ancient technology is needed to be used for developing elevation model and the uncertainties should be minimised to make it suitable for flood modelling.

3. Study Area and Data Pre-processing

3.1. Introduction

This chapter provides the details of the study area and the data available for analysis. It will provide an illustration of the location and geography of the study area. The chapter will also include the description of the steps involved in the pre-processing of the data.

3.2. Study Area

The study area was situated in the Gelderland province of the Netherlands, which is in the south-eastern part of the country near the border with Germany. Here the river Rhine bifurcates after entering the province. The main part of the river is flowing to the north with the original name, while the other part, the distributary of the river, is flowing westward under the name Waal. The exact location of the study area (Figure 3-1) was in the flood plain of the river Waal. The spatial extent of the study area was from 51^0 52' 57" N and 5^0 59' 45.26" E to 51^0 52' 40.26" N and 6^0 02' 24.18" E in the north and from 51^0 51' 33.18" N 5^0 58' 53.97" E to 51^0 51' 09.15" N 6^0 01' 01.95" E in the south. Total 8.37 km^2 area was present under the study area. The average height of the area was 12m above mean sea level. A temperate maritime climate prevails in the Netherlands and the same prevailed in the study area. The rainfall was evenly distributed throughout the year and the average annual precipitation was about 700 mm.

3.3. Available Data

3.3.1. Aerial photos

The main data source that was used for this study was the aerial photos of the study area. All the photos were captured using a RMK TOP 30 film camera during June 2005 and later on scanned to obtain the digital photo. A total of 11 photos comprise the area, which includes 6 images in the first strip and 5 in the second strip.

3.3.2. Orthophoto of the Area

The orthophotos were available as false colour composite (3 layers) and had a spatial resolution of 0.25 m. It was projected in RD-NAP projection system. These orthophotos were used to collect the ground control points for triangulation.

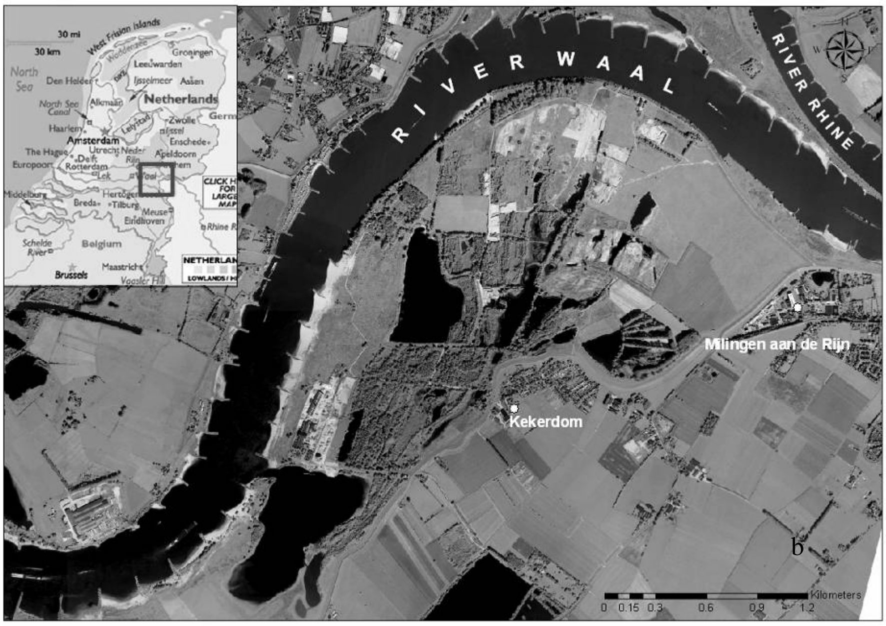

Figure 3-1 Map showing the study area in orthophoto

3.3.3. Digital Terrain Model from LiDAR data

The DTM was provided by the Geo-information and advisory service ICT and it was prepared maintaining the specification of Actueel Hoogtebestand Nederland (AHN) 2000 system. It was developed from a LiDAR base file with an average dot density of 1 point per 16 m^2, being denser in open areas and comparatively less dense in vegetated areas. The vegetation and buildings were subsequently removed from the LiDAR data using filtering techniques. The inverse distance squared weighting interpolation method was used to generate the continuous height model in regular 5m X 5m GRID format. The projection system was the native RD/NAP projection system for the Netherlands. Planimetric accuracy of the model was better than 30 cm The details of the errors in the DTM are given in Appendix C1. Although a LiDAR derived DTM was already available for the study, the aim of the study was to assess the potential of the aerial photos, which were very old and widely available data, for DTM generation. Thus the LiDAR DTM was only used to assess the accuracy of the DTM derived using aerial photographs.

3.4. Preprocessing of the aerial photos

The raw aerial photos were pre-processed using photogrammetric techniques to obtain the pseudo DTM. Photogrammetry involves the establishment of the relationship among the photos as well as between the photo, the camera and the earth's surface, which rectifies the photo to the appropriate characteristics of the earth's surface. Each of these variables (camera, photo and earth's surface) should be defined with respect to plannimetric and vertical coordinate system in the image space. Before carrying out the pre-processing steps a ***.blk*** file was created in Leica Photogrammetric Suit (LPS) which collected all the information such as camera specifications, calibration parameters and GCP measurements. During this step the preferred projection was chosen as the same projection of the LiDAR DTM file i.e. RD-NAP. For the pre-processing of the aerial photo the standard method described in the manual of LPS was adopted. Each of the steps followed are briefly described below.

3.4.1. Image rotation

The available data included the 11 aerial photos in two strips. Initially the original images (Figure 3-2A) were with north facing down and they were used without rotating them. The orientation parameters were also specified accordingly.

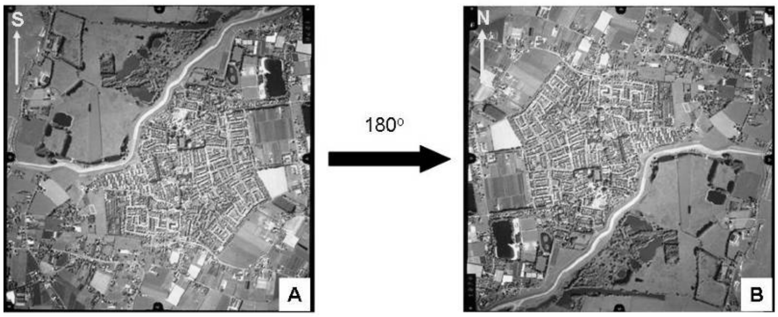

Figure 3-2 (A) The original image and (B) image after rotation by 180 degree

During automatic image matching process no match points were found amongst first three pairs of images of the two strips. Thus later on the images were rotated by 180° with north facing up (Figure 3-2B) to facilitate further processing and the image matching process was carried out successfully.

3.4.2. Interior orientation

The internal geometry and the characteristics of the camera at the time of image capture are defined by the interior orientation of the sensor model. It is required to transform the image coordinate system to the image space coordinate system. For a frame camera this process requires the focal length of the camera, the principal point in the image plane, the fiducial marks and the lens distortion statistics. These information were collected from the camera calibration certificate (Appendix C2) and accordingly applied in the course of process.

3.4.3. Exterior orientation

The position and the angular orientation of the camera were described by the exterior orientation of the camera. Three positional (X_o, Y_o, Z_o) and three angular (ω, κ, ϕ) independent elements were calculated in this step. The rotation angles were used to establish the relationship between image space coordinate system and the ground space coordinate system. These values were also supplied with the camera calibration information as a ***.dat*** file and the values were used as initial values to perform the exterior orientation and derive the final values for the orientation parameters (X_o, Y_o, Z_o and ω, κ, ϕ) for the images.

3.4.4. GCP measurement and automatic tie point generation

GCPs and check point were collected using the existing orthophoto and the LiDAR DTM. Both data being in the same projection system it was possible to identify the suitable points in the orthophoto and collect the X, Y and Z for the same points in the LiDAR DTM. Arc GIS 9.2 was used for this purpose where both data sets were overlaid and GCPs were collected manually. All GCPs were collected at road intersections, field corners and in areas with recognizable pattern.

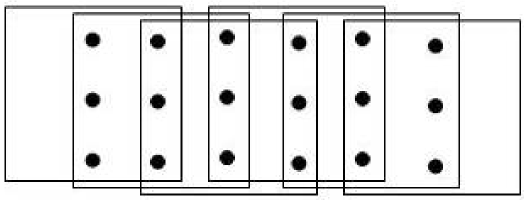

Figure 3-3 GCP Collection Strategy

At least 6 GCPs were collected for each overlap area between two successive photos following the strategy shown in Figure 3-3. 100 tie points were automatically generated using the in-built function in LPS. Prior to that 4 tie points were manually placed per image pair to facilitate the triangulation process in the next step.

3.4.5. Block triangulation

Block triangulation is a method of building a mathematical relationship among the images in a block, the camera and the ground. Among the most widely used block triangulation methods, the independent model method and the bundle adjustment are commonly used. Bundle block adjustment is the most rigorous and efficient method in terms of error distribution (ERDAS, 2008). The basic theory of bundle block adjustment is based on the most elementary unit of photogrammetry, which is the image ray. An image results from this bundle of rays which converge in the perspective centre of the image at a particular orientation. Using the given GCPs, the bundle block adjustment establishes the position of the centre and the orientation of the bundle of rays. This process is based on the collinearity equations (Mikhail *et al.* 2001). The bundle block adjustment was carried out for the block of images of the study area using the GCPs and tie points. Initially a relatively larger error in the adjustment result was encountered. The error was minimised interactively by checking the positions of the GCPs and the tie points. The erroneous tie points were removed and the block was re-triangulated each time after editing. The overall triangulation error (in RMSE) was calculated as 0.6127 pixels. The ground X, ground Y and ground Z RMSE were 0.2873, 0.3642 and 0.4205 respectively. The triangulated block of images was then used for automatic extraction of elevation model. The photogrammetric image processing operations inherently carry some systematic errors due to lens distortion, camera distortion, scanning process and atmospheric refraction, which were also included in the triangulation errors.

3.4.6. DSM extraction and Orthophoto generation

The DSM was generated automatically using the triangulated block of images in the grid format. The cell size of the DSM was specified as 5 m X 5 m. The DSM was generated as a single mosaic for all the areas having more than 30% overlap. A contour map with 2 m interval was also generated along with the DSM. Orthophotos were generated for each of the images in the block using the DSM as the source. Two sets of orthophotos are generated having cell resolution of 0.25m and 5m.

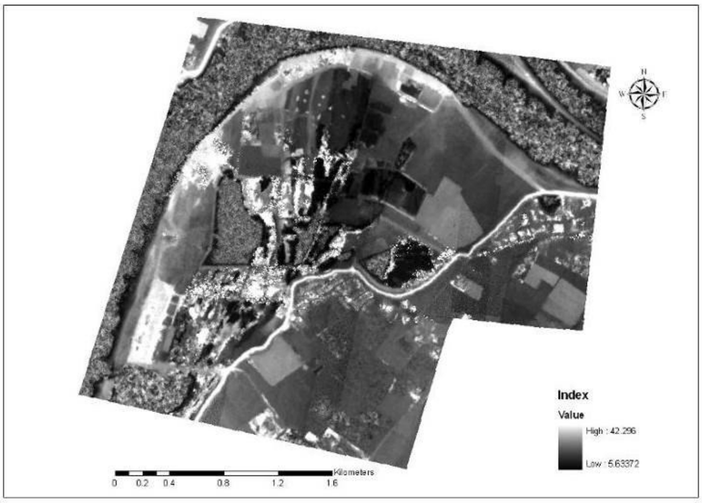

Figure 3-4 DSM of the study area in the southern part of the River Waal

The same projection system as for the LiDAR DTM (RD-NAP) was specified, and nearest neighbourhood interpolation was used to generate the orthophotos. Initially the DSM and the orthophotos were generated for the total area covered by 11 stereo pairs (Appendix D1). Later on, keeping in mind the practical and technical feasibility in further analysis, the study area was limited to the flood plain in the southern part of the river Waal (Figure 3-4)

3.4.7. Accuracy Assessment of the DSM

The accuracy of the DSM was carried out comparing its heights with the LiDAR DTM at the GCP locations. Figure 3-5 shows the distribution of the errors in height at the GCP point locations. The majority of the GCP locations showed an error within ±0.5 m, though very few exceptions were there. The overall RMSE was calculated as 0.122m.

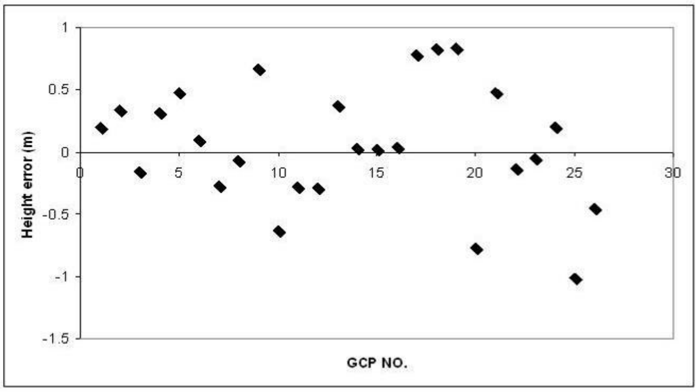

Figure 3-5 Distribution of error in height in A-DSM at the GCP locations

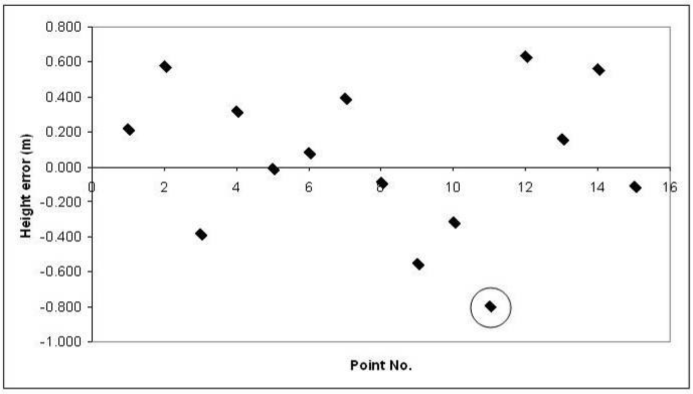

Figure 3-6 Distribution of error in height in A-DSM at independent locations

The accuracy of the DSM was also estimated by comparing its heights with the LiDAR DTM at 15 independent point locations. Figure 3-6 shows the distribution of error in height in the DSM at the independent locations. The majority of the errors were also within ± 0.5m with few exceptions. The overall RMSE was estimated as 0.107m.

All of the independent check points are located on the bare earth surface. In the areas with landcover features such as buildings and vegetation, the height differences between LiDAR DTM and DSM were much higher than the range mentioned above. This was because the LiDAR data depicts the height of the bare earth surface i.e. without surface features (i.e. a DTM), whereas the DSM includes the surface features on it.

3.5. Errors in the orthophotos

Apart from typical systematic errors in photogrammetric image processing, there were some inherent errors in the source data. The two strips of data were captured in different time. Though the time and date is not present in the scanned photos, because they might be ignored during scanning, but the difference in the water level in the coastal area proves the fact of different time of photo acquisition. This resulted in some differences in the features in the two strips of images. (Figure 3-7).

Figure 3-7 Error in coast line due to difference in image acquisition time

3.6. Summary

This chapter thus provided the available dataset and the methods followed to generate the DSM and the orthophotos using those data. The chapter also demonstrated the error estimation process and focused on the errors present in the derived DSM and the orthophotos. Quantification of these errors was important because the data derived here were the main input for the further analysis and the error present in them can potentially influence the results in further analysis.

4. Methodology

4.1. Introduction

In continuation of the previous chapter, two dataset are now available for further analysis to determine the DTM suitable for flood analysis. These are the DSM and the orthophoto. The aim of this chapter is to show the different options to eliminate obstacles from the DSM. The first part is on feature identification, the second is on feature removal.

4.2. Feature extraction techniques from aerial photos

As mentioned earlier, the aim of the study was to develop a pseudo-DTM suitable for flood risk assessment. Two step processes was required: (1) identification of the features on the DSM and (2) correction of the DSM. Two major approaches were available for this purpose namely pixel based and object based approach. This research was carried out by undertaking the pixel based approach for feature identification, to limit the scope of the research. Considering the available dataset the potential information of the orthophoto that can be used for this analysis were colour and texture of landcover features.

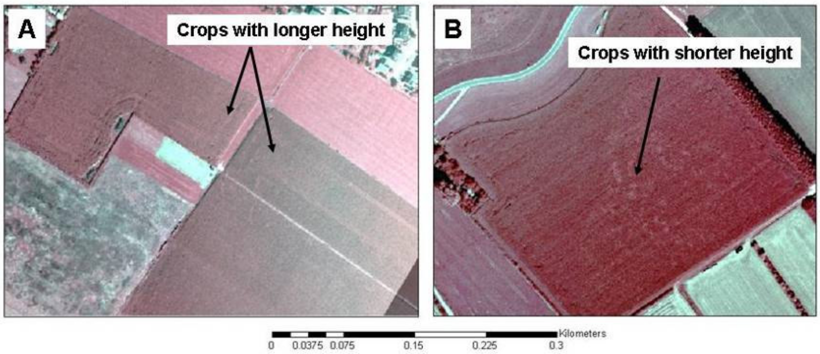

Figure 4-1 Agricultural lands in the study area: (A) crops with longer height and (B) crops with shorter height

The discussion in chapter 2 made it clear that at a particular resolution some of the surface features act as obstacles (e.g. buildings and dikes) to the water flow and some do not (e.g. broadly vegetation). However, in a DSM, the permeable obstacles

also appear as impermeable and thus they should be removed for more accurate flood risk analysis. In this connection it is necessary to clarify that all vegetation sub-classes do not really appear same on the DSM. For example trees, bushes and agricultural crops act as impermeable obstacles in a DSM whereas grasses do not because the former group of vegetation grow comparatively much higher than the later. Moreover, precisely all the agricultural crops are not obstacles either. Crops like maize which can grow up from 2.5 m to 7 m can well appear as an obstacle in the DSM. On the contrary, crops such as potatoes and beans having height less than a meter do not really appear as obstacles (Figure 4-1).
The study area consisted of 5 main landcover classes and their sub-classed as depicted in Figure 4-2.

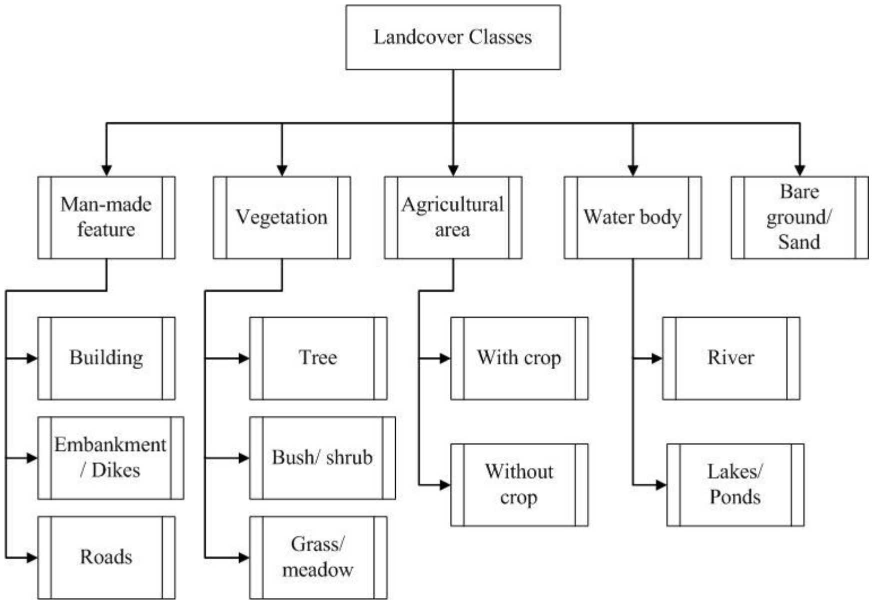

Figure 4-2 Landcover classes and sub-classes in the study area

Considering the literature review in chapter 2, the terrain characteristics and the landcover features present in the study area, the research decided that for low and medium intensity flood the trees, bushes and crops with greater height should be removed while the man made features (e.g. buildings, dikes and embankments), water body and grass land including crops with lower height should be kept in the pseudo-DTM.

Therefore, the research focused on the identification and removal of vegetation sub-classes such as trees, bushes and crops with greater height from the DSM, which also implies accurate identification of non-vegetation classes as well as other vegetation sub-classes such as grass and crops with lower height to retain. Table 4-1 shows the different landcover features to be removed and retained. In Table 4-1 the landcover feature named as "agricultural area with crop" indicates the crops with comparatively longer height and the crops with shorter height were included in the features named "grasses/meadows".

Table 4-1 Landcover features needed to be removed from the DSM and retained in the DSM

Landcover features	Retain	Remove
Building	√	
Embankment	√	
Dike	√	
Tree		√
Bush		√
Grass/ Meadow	√	
Agricultural area with crop		√
Agricultural area without crop	√	
Lake / Pond	√	
Bare ground / Sand	√	

Considering the potential properties of the available dataset for this analysis, the correction of DSM was done using two methods.

1. Identify and delineate the features on the orthophoto using colour and texture of the features and use it as a mask to apply on the DSM to identify the features, delineate their extent on the DSM and remove them from the DSM.

2. Identify the features on the orthophoto using their colour and texture and also identify the features on the DSM by linking the orthophoto and the DSM logically (using co-ordinate system), then delineate the features on the DSM and remove them from the DSM.

4.3. Proposed Approach for the Study

As discussed earlier, the study concentrates on the identification of the surface features and removal of trees, bush and crops from the DSM retaining all other surface features (Table 4-1) on the DSM. Thus the process needed accurate identification of different landcover features (especially vegetation sub classes). This required advanced image analysis techniques and accuracy assessment to ensure the reliability of the derived product for further analysis on flood risk management. Only one software package does not always have all required image processing functions. Therefore, to bridge the gap and to execute the best analysis results, the following software tools were used in this research.

- ERDAS imagine (9.2) for image classification, accuracy assessment and post-classification analysis.
- ENVI (4.5) for texture analysis.
- Arc GIS (9.3) for post-classification analysis and database generation.

To ensure easy transferability of data among different software the projection system of the data was changed to UTM (Zone 31) with a datum of WGS 84.

4.3.1. Feature Identification

The study area was broadly categorised in 5 different landcover classes (Figure 4-2). These features can be identified in the orthophoto using pixel based classification using their colour and texture characteristics individually or as combination of both. However, distinguishing different vegetation types (trees, bushes and grasses) on the basis of colour and texture is always challenging, because the different types of vegetation do not always show different colour and texture pattern. The effect of shadow again increases the confusion. For the first approach the following methods was used.

Option 1: classification based on colour

As the orthophoto was a false colour composite of three layers (red, green and blue), different landcover classes show distinct colour variation. This property of the orthophoto was used to build up training sets for supervised classification on it. Keeping in mind the purpose of the study, 6 different landcover classes which were selected to classify the image were (1) building / road, (2) crop / bush /tree, (3) agricultural land without crop, (4) meadow (5) water body and (6) bare ground / sand. 10 training sets were created on the orthophoto for each landcover class. The supervised classification was carried out using the training sets and maximum likelihood classification algorithm was used for this purpose.

Although the 5 broad landcover classes shown in Figure 4-2 have distinct colours, all the areas are not homogeneous. Clearly delineated areas as seen in Figure 4-3 (A) are likely to be more precisely classified than areas depicted in Figure 4-3 (B). As the colour of grasses and trees was similar it was difficult to distinguish them. Especially in the transitional areas the segregation of the trees from the grasses was more difficult due to presence of different combination of landcover classes. Similarly bare agricultural field and the adjacent roads (Figure 4-4 A) and roofs of buildings and sandy area (Figure 4-4 B) had same colour which made the classification process more complex.

Figure 4-3 (A) Homogeneous forest with only trees and (B) mixed forest with trees, bushes and grasses in the study area

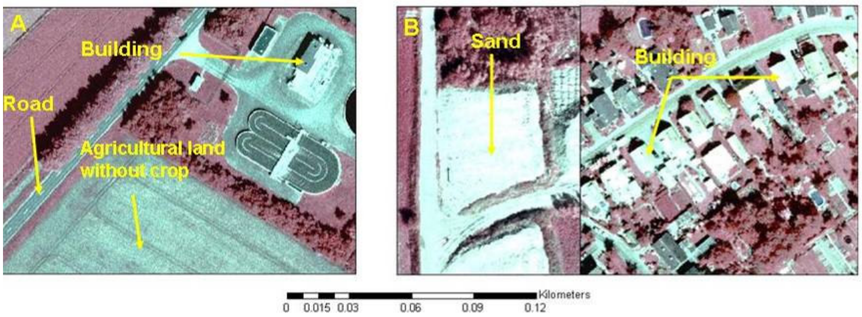

Figure 4-4 (A) Agricultural field beside road and (B) sand and roof of buildings in the study area

<u>Option 2: classification based on texture</u>

Texture analysis was widely used in different studies for identification of different landcover features, especially in very high resolution images such as aerial photos

(Hudak and Wessman, 1998, Lovan *et al.*, 2007, Caridade *et al.*, 2008, Ge *et al.*, 2006, Franklin *et al.*, 2000, Zhang *et al.*, 2003b, Baillard *et al.*, 1998). Texture analysis can be done using the GLCM (for details see chapter 2) and then the measures can be used as additional bands in the subsequent pixel based image classification process.

The texture statistics were calculated in the red layer of the two sets of orthophoto (0.25m and 5 m resolution). The red layer was chosen here because it provides the best contrast amongst all 3 layers. Seven texture parameters which were used in this study were mean, variance, homogeneity, entropy, angular second momentum, contrast and dissimilarity. The inbuilt texture algorithms of ENVI 4.5 were used (Appendix D2). Since some part of the study area was homogeneous (e.g. meadow and forest) and some part was heterogeneous (e.g. settlement with vegetation) texture parameters were calculated for 6 different window sizes (3 X 3, 11 X 11, 27 X 27, 35 X 35, 43 X 43 and 71 X 71) for orthophoto of cell resolution 0.25m. The largest window size was decided by measuring the average tree crown diameter on the orthophoto. Since the resolution of the orthophoto was very high (0.25m) large window size was taken into consideration to calculate the variability of the texture statistics especially in the homogeneous area. For the orthophoto of 5m cell resolution texture variance was calculated using only 3 X 3 search window.

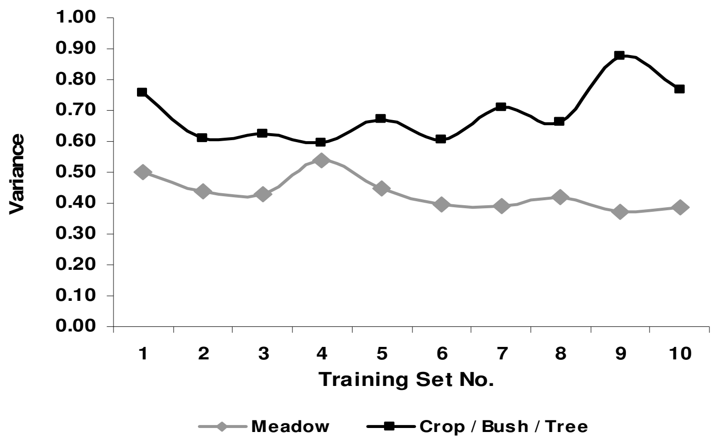

Figure 4-5 Frequency distribution of texture variance of meadow and crop/bush/tree class

To determine the most suitable texture statistics among all 7 statistics, the signature of 7 different landcover features were determined by creating 10 training sets for each landcover class and they were plotted graphically to understand the inter-class separability. From the analysis of frequency distribution of different texture statistics over the area (Figure 4-5 and Appendix D3 – D8), it was found that among the 7 texture statistics only variance can clearly segregate meadows and areas with tree, bush and crop (Figure 4-5). However, the texture variance of other classes considerably overlaps with each other as well as with both the vegetation subclasses (Figure 4-6).

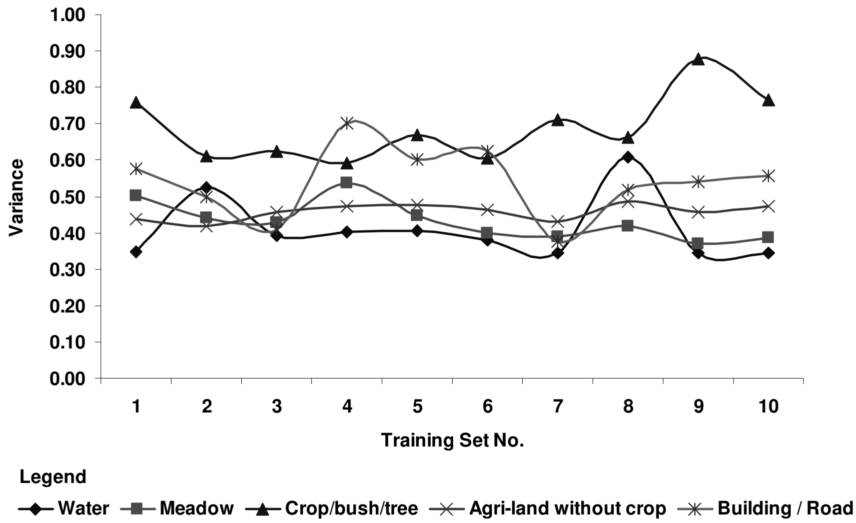

Figure 4-6 Frequency distribution of texture variance of different landcover features (using 10 training sets)

This overlapping class signature of the landcover classes will ultimately lead to misclassification. Therefore, only texture property of the landcover features was not sufficient to segregate all the features precisely. There was a need of an integrated classification process considering both the texture and the colour properties of the landcover features.

<u>Option 3: classification based on both colour and texture</u>

Classification based on both texture and colour can be more efficient than using both the measures individually. All the texture measures can be used as additional bands along with the standard RGB during classification process. Several studies have used colour and texture together to identify features (Caelli and Reye, 1993, Ge *et al.*, 2006). On the contrary, Maenpaa and Pietikainen (2004) concluded from their results that colour and texture are two separate phenomena and should be treated separately.

The combined colour and texture analysis was done in two different methods. The first method used the colour and the texture together and the other used them as separate properties. These analyses were done using two type of cell resolution of the orthophoto (0.25m and 5m).

First the colour texture images were derived in three layers for both the orthophotos (0.25m and 5m). 6 different window sizes (mentioned earlier) were used to calculate texture variance for the orthophoto with 0.25m spatial resolution and only one for the orthophoto with 5m spatial resolution. Supervised classification was then performed on the colour-texture image into the 6 pre-defined classes on all the coloured texture images. As 0.25 m orthophoto was in greater details, to save the computation time and for technical feasibility, a representative subset of the study area was chosen to perform the operations (Figure 4-7).

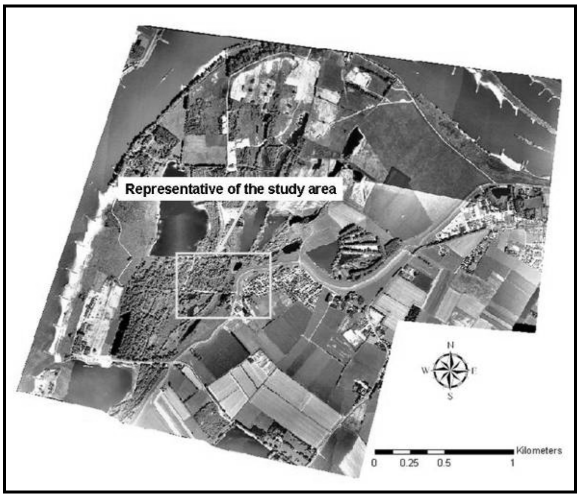

Figure 4-7 Representative study area for classification of orthophoto based on colour and texture

Prior to the classification the class separability was verified by plotting graphically the frequency distribution of different classes considering 5 training sets for each class in the study area. From the signature pattern (Figure 4-8) it was clear that the meadows and crop / bush / tree class can be differentiated quite clearly. Although it was possible using only texture, but this method additionally can segregate the other classes from crop / bush / tree class. The overlapping signature of meadow with water, shadow, bare ground / sand and agri-land without crop was ignored as they all would be retained in the pseudo-DTM. Figure 4-8 shows that the signature pattern of the crop/bush/tree class covers a wide range of variation. This class represents the texture variance of tree, bushes as well as of crops. All three vegetation sub-classes may have different texture pattern. In some cases, crops, depending on the type, have smoother texture similar to grasses while some other crops may have same texture as trees. As the landcover, especially vegetation, in this area is not homogeneous the texture variance of vegetation is more variable compared to the other classes.

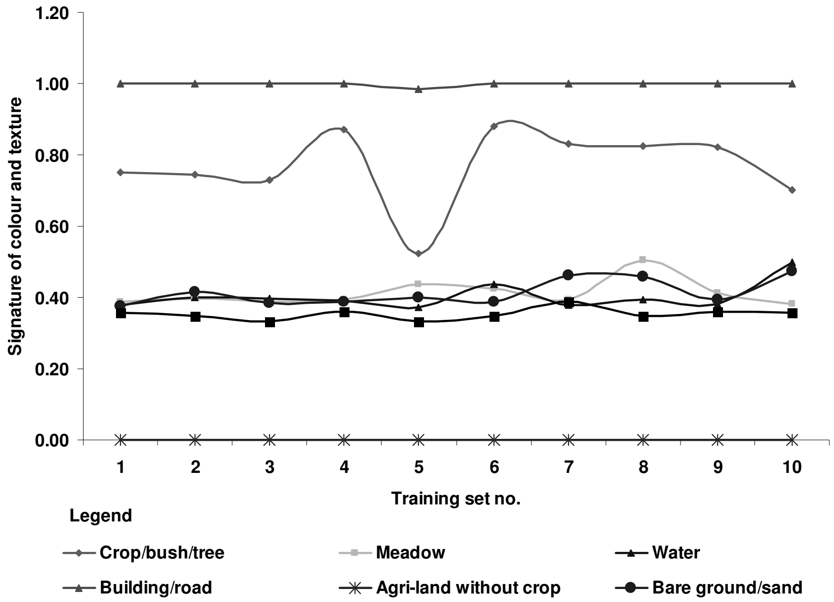

Figure 4-8 Graphical representation of the frequency distribution of colour and texture variance of different landcover features in 5m orthophoto (using 10 training sets)

The second method used the colour and texture of orthophoto as separate entities. In this method, at first supervised classification was carried out on the orthophoto with colour only. The image was classified in to vegetation and non-vegetation classes. This classified image was then recoded assigning vegetation as "1" and non-vegetation as "NoData". The texture variance was derived in only 1 layer of the orthophotos in this case, because all the bands contain similar texture information (as it is a scanned image). The red band was again chosen for texture calculation. The texture image was then masked with the recoded classified image to obtain the texture variance of only vegetation subclasses. A schematic diagram of the classification method is depicted in Figure 4-9.

4.3.2. Accuracy Assessment of classification

The accuracy assessment was undertaken for each of the classified images. The error matrix and kappa statistics were calculated in ERDAS imagine quantifying the error. The error matrix compares the relationship between known reference data and the corresponding classified data. For each of the classified images 200 random points were generated on the classified data and the classes of the points were cross checked using the reference orthophoto. Kappa statistics (k) was also calculated for the classified images using the following equation (Lillesand and Kiefer, 2002).

$$k = \frac{N \sum_{i=1}^{r} x_{ii} - \sum_{i=1}^{r} (x_{i+} * x_{+i})}{N^2 - \sum_{i=1}^{r} (x_{i+} * x_{+i})} \quad \ldots\ldots\ldots\ldots\ldots\ldots\ldots\ldots\ldots\ldots \text{(i)}$$

Where,

r = no. of rows in the error matrix.

x_{ii} = no. of observation in row i and column i (major diagonal).

x_{i+} = total observation in row i.

x_{+i} = total observation in column i.

N = total no. of observation in the matrix.

4.3.3. Feature removal

After identifying the features in the image, it is necessary to find out the features on the DSM and remove them from it. The methods which were used for feature removal are described below.

Option 1: Binarisation and Interpolation

Binarisation and interpolation method was adopted from the study by James *et al.* (2006). In this process the classified coloured texture images were recoded to a binary image with trees / bush / crop class as “NoData” and other classes as “1” using Arc GIS software package. The Binary image was then multiplied with the DSM. This process removed the height information from the pixels in the DSM with tree /bush / crop class. Finally, inverse distance weighted (IDW) interpolation was used to create a continuous surface by filling the “NoData” pixels with the height value from its surrounding pixels. The k value for IDW was taken as 2. The process is depicted in Figure 4-10.

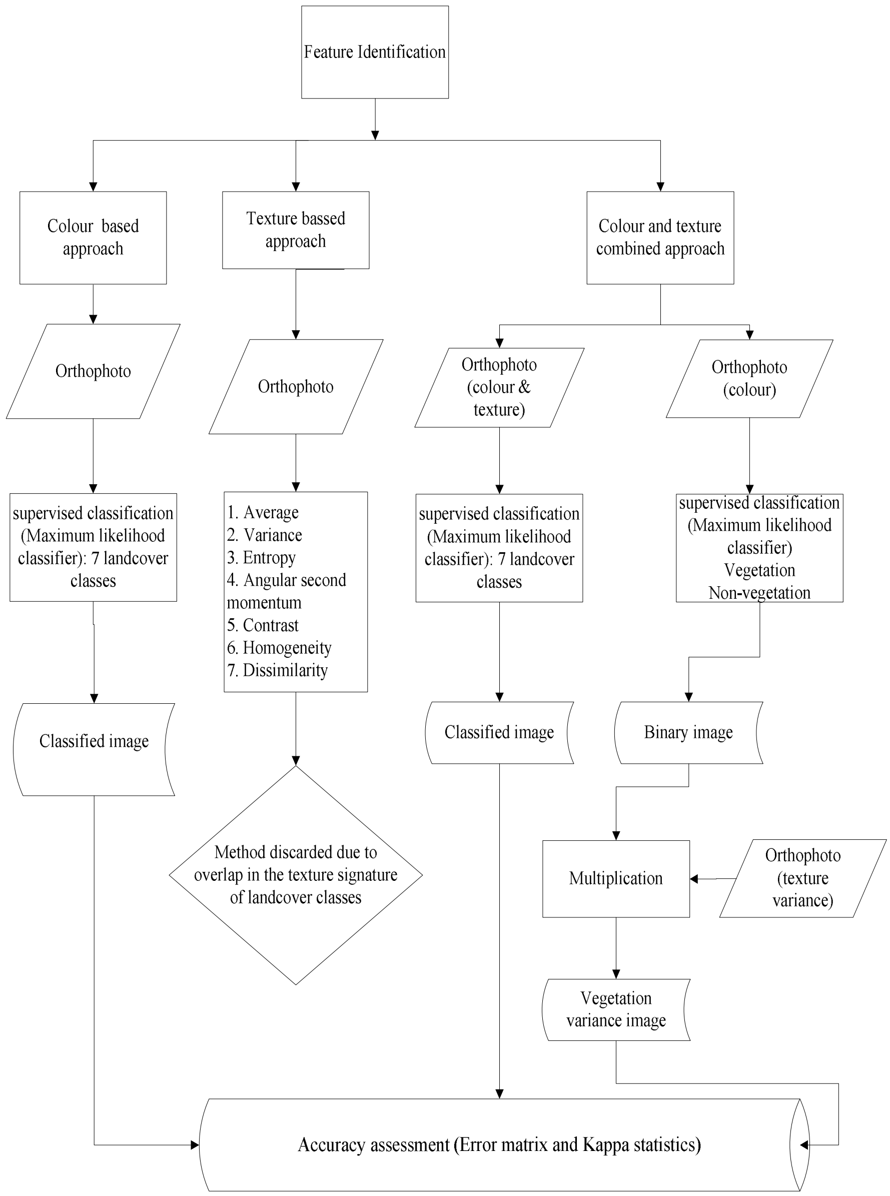

Figure 4-9 Schematic representation of the feature identification method

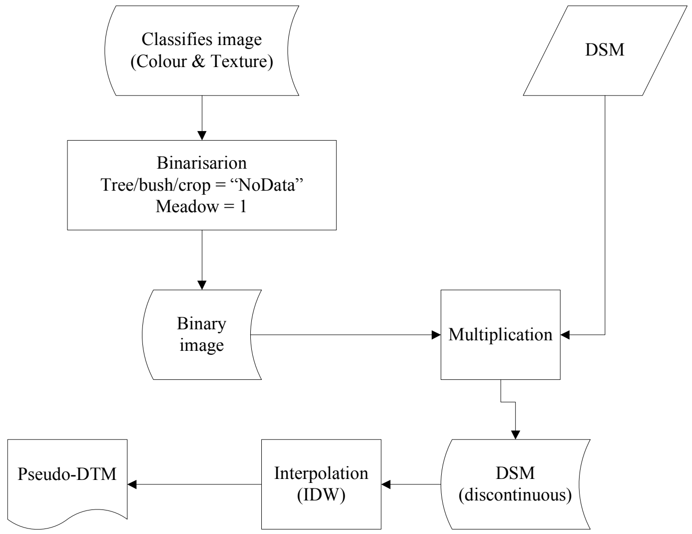

Figure 4-10 Schematic representation of the binarisation and interpolation process

<u>Case: 1</u>

In an ideal scenario (Figure 4-11) where the vegetation has distinct variation either in colour or in texture with all surrounding classes, it is easy to delineate the boundary of the vegetated area from the other classes. This method may work satisfactorily.

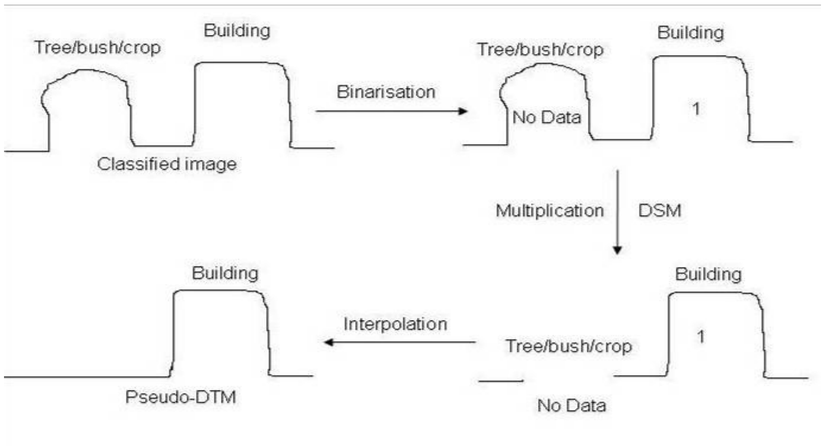

Figure 4-11 Pseudo-DTM generation in case 1

Case: 2

However, it is very rare that all the vegetation is perfectly classified all over the area. It is frequently found that different landcover classes have same colour and textural pattern (Figure 4-3 and 4-4). Always there are cases of misclassification in those areas which lead to error in generating DTM using the binarisation and interpolation method. In that case the classification will not result in smooth and clear cut edges between different classes and the final product will be erroneous (Figure 4-12).

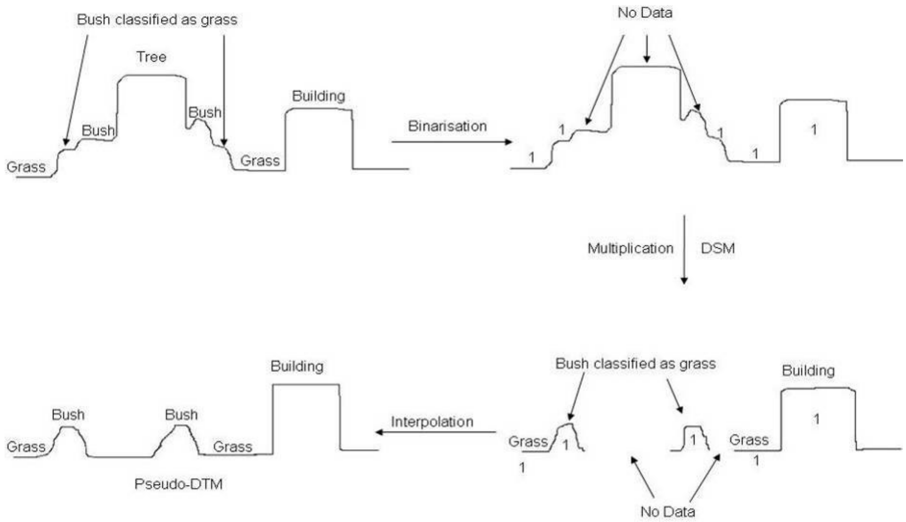

Figure 4-12 Pseudo-DTM generation in a complex landcover area (case 2)

Case: 3

There are some dikes which are covered by vegetation and some sudden depression under the vegetation present in the study area (Appendix E1). In aerial photo it is not possible to identify such sudden changes in the topography covered by vegetation. The bumps and the depressions act as obstacles and sinks respectively for water flow. Using the binarisation and interpolation method the dike and the depression as will not be accurately described in the resulting pseudo-DTM. Figure 4-13 shows the pictorial representation of the situation. If so, then the flood model will not predict the flood situation correctly. No doubt the impact of these errors depends on the scale of flood occurrence (see Chapter 2).

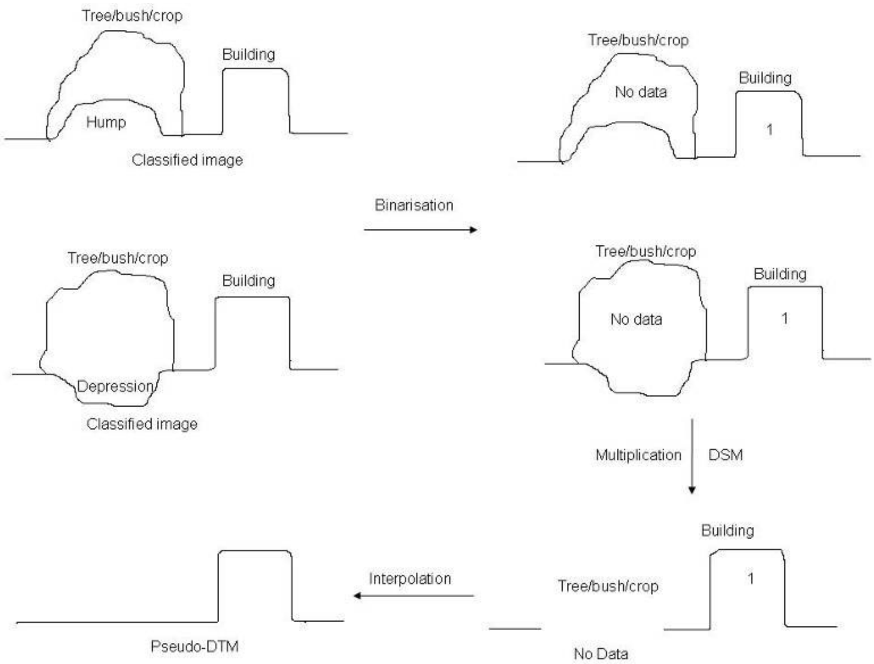

Figure 4-13 Pseudo-DTM generation in case 3

Option 2: neighbourhood analysis

Neighbourhood analysis is frequently used in filtering especially laser elevation data. Vosselman (2000) proposed a slope based filter to segregate the ground and non-ground points by comparing the slope between the neighbouring points. Morphological filters are also commonly used to remove non-ground measurements from laser data (Zhang *et al.*, 2003a, Chen *et al.*, 2007).

The second method used for feature removal from the DSM was neighbourhood analysis on the DSM based on the filtering methods. This process analysed each and every pixel spatially using the pixels surrounding it within the scanning window. For the neighbourhood analysis the “vegetation variance image” (Figure 4-9) and the DSM were used. A logical model was developed in ERDAS model maker. The model was considered for two input data and a matrix (Figure 4-14). The size of the matrix was determined as 35 X 35 by simulating the model several times with different window size. This window size was found to be the optimum for this particular area. A function was written in the model maker which searches all the pixels on the DSM to find the focal height minima of the areas where the variance in texture greater than 0.55. The threshold in texture variance was derived from the frequency distribution graph (Figure 4-5). After the model found those pixels fulfilling the condition, the height value of the pixel was programmed to be replaced by the minimum height value within the window (Figure 4-15).

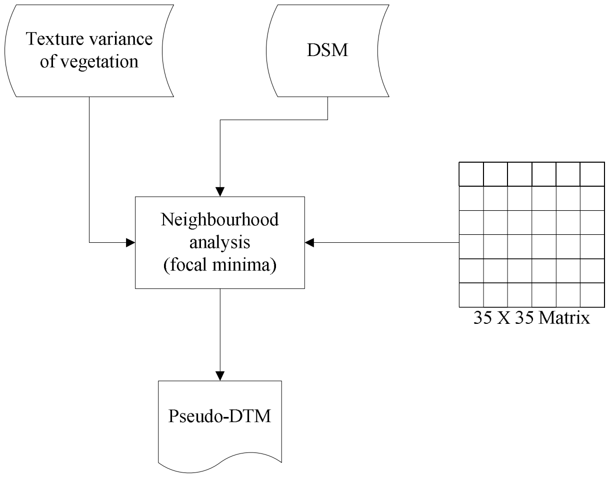

Figure 4-14 Schematic representation of neighbourhood analysis

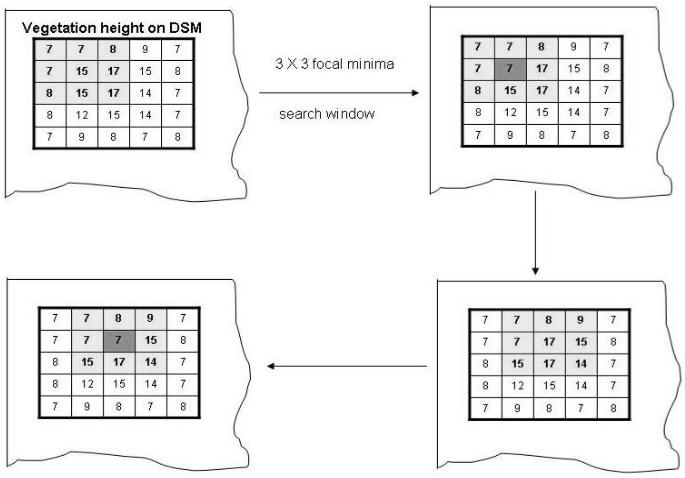

Figure 4-15 Focal minima calculation using neighbourhood analysis

On the DSM each of the buildings and vegetation (excluding grass) appear as humps because of height difference from its surroundings, though photogrammetrically derived elevation model does not depict clear edges. The search window was functioned to find the minimum heights among the pixels in the window and replace the height of the centre pixel with the minimum height. This region growing process continued through all the pixels in the DSM. As the source data for this analysis only contained the vegetation classes the programme only could search for the vegetation classes to find the texture variance and change the height in those areas Therefore, the areas with non-vegetation landcover classes, the height value were supposed to remain same as in the DSM.

For case 1 and case 2 (Figure 4-11 and 4-12) in this study, this method may work better than the previous method. Since the neighbourhood analysis is carried out on the DSM, misclassification during feature identification will affect the tree, bush and crop removal process less than it does in binarisation and interpolation method. The search window identifies the features using the texture description and reduces the height of features in the corresponding areas in DSM. However, in case 3, this method fails as well. Since the search window always compares the top of crown height with the immediate ground height, any sudden bump or depression will be smoothened during the removal process. Another reason for failure is the type of data under consideration. Unlike laser data, the aerial photo does not provide the ground information in locations covered by any landcover feature (e.g. vegetation).

4.3.4. Accuracy assessment of the pseudo-DTM

The accuracy assessment of the derived pseudo-DTMs was carried out qualitatively and quantitatively. In this regard the LiDAR DTM was considered as the reference data. Both the DSM and the derived pseudo-DTMs were compared with the LiDAR DTM.

In the first stage, the pseudo-DTMs were compared with the DSM to find out the extent of correction. In this regard, the change detection images were calculated for the areas in the pseudo-DTM with changes in height by more than 10% from the DSM using change detection function in ERDAS.

In the second stage, the errors in the DSM and the derived DTMs were calculated by means of difference image between the DSM and LiDAR DTMs and the pseudo-DTM and LiDAR DTM. The subtraction of the LiDAR DTM from DSM and pseudo-DTM estimates the magnitude and the spatial distribution of the height errors. The mean of the residuals and standard deviation of the residuals from the mean were measured for the whole study area.

In this regard it was important to notice that the LiDAR DTM did not contain any surface features on it except the embankments and roads while DSM had all the surface features present on it. The pseudo-DTMs have all other surface features except crop, bush and vegetation. Therefore, the height will be substantially different in areas with other landcover classes (especially with buildings) and in the difference image it was expected to find high errors in these areas. Obviously, in this case, the mean of the height residuals was expected to be a non-zero number and the standard deviation to be quite high.

In the last step, to evaluate the efficiency of the correction routine, the areas with only crop, bush and tree were masked out from both the pseudo-DTM and the LiDAR DTM. The error in height was then measured by subtracting the LiDAR DTM from the pseudo-DTM. The mean and standard deviation of the residuals were again calculated

4.4. Summary

This chapter provides the details of the image analysis process undertaken in this study. The chapter also includes some previous works that was done for similar analysis to support the methodological approach. The methods were also analysed here with respect to three scenarios to provide some expected outcome of the methodology. Finally, the chapter focuses on the methods of accuracy assessment that was carried out to assess the efficiency of the method and the accuracy of the pseudo-DTMs.

5. Results

5.1. Introduction

The accurate characterisation of the earth's surface and the features on it facilitates efficient and accurate flood risk prediction and management. The advent in remote sensing generated high resolution images (space borne and air borne) which has made this process of characterisation of the surface topology much easier. Broadly, this process can be carried out either using pixel based analysis or objects based analysis. However, many studies follow a combination of both the approaches (Lu *et al.*, 2006, Baillard *et al.*, 1998, Lovan *et al.*, 2007) .

Within the scope of this study, only pixel based approach was taken into consideration. The entire method was divided in to two parts namely identification and removal of the features. To identify features, the orthophoto was classified using colour based and texture based methods. Likewise, two approaches were carried out to remove the features from the DSM.

5.2. Feature identification: classification results

5.2.1. Option 1: classification based on colour

The first phase of classification was carried out with the orthophoto considering only colour of the landcover features using maximum likelihood classification algorithm. The accuracy assessment of the classification was performed in ERDAS 9.2 by generating 190 random points in the classified image and comparing the classes with the available orthophoto. The summary of the classification is shown in Table 5-1.

It was evident that the classification accuracies were very poor for all the landcover classes except water. Especially for tree/bush/crop and meadow classes both the error of commission and error of omission were high. This indicated the poor efficiency of the process to separate those landcover classes. The overall accuracy of the process indicated that only 58.9% of the landcover features was classified accurately. The kappa coefficient provided more detail assessment of the quality of the classification as it also considered the agreement "by chance" between the reference data and the random classifier along with the "true" agreement. Here low value of kappa indicated the percentage of chance agreement was quite high. From the error matrix it was clear that majority of the misclassifications occurred between the sub-classes of vegetation.

Table 5-1 Error matrix for classification results of orthophoto based on colour

Classified data	Reference data						
	Crop / bush / tree	**Meadow**	**Building / road**	**Bare agri-land**	**Bare land / sand**	**Water**	**Sum**
Crop /bush/tree	**28**	37	0	0	0	1	66
Meadow	12	**21**	0	0	0	0	33
Building / road	0	0	**3**	1	0	6	10
Bare agri-land	3	0	0	**11**	6	1	21
Bare land / sand	0	0	2	2	**10**	0	14
Water	3	1	1	1	1	**39**	46
Sum	46	59	6	15	17	47	190
Producer's accuracy	60.9%	35.5%	50%	73.3%	58.8%	82.9%	
User's accuracy	42.4%	63.6%	30%	52.4%	71.4%	84.7%	
Overall accuracy	58.9%						
Kappa	0.47						

Although this classification method could not segregate the vegetation sub-classes from each other, it could differentiate the vegetation and non-vegetation features quite efficiently. This can be interpreted from the error matrix where it was clear that there were not may other class pixels which were classified as vegetation as a whole. If vegetation sub-classes were combined in to a single class the overall accuracy would increase to 84% and accordingly the kappa to 0.76 which were substantially better than the previous result. Thus there was a need of second level classification to differentiate the vegetation sub-classes. It was important because in the DSM the meadows should be retained as it was whereas the tree, bush and crops should have been removed from it to obtain the pseudo-DTM. Due to poor value of kappa and high error of commission and omission between crop/bush/tree and meadow class no further analysis with this data was carried out.

5.2.2. Option 2: classification based on texture

Although the texture variance could segregate the crop/bush/tree and meadow classes, there was substantial overlap of texture variance signatures of other landcover classes with those two vegetation classes (Figure 4-6 and Appendix F1). Therefore, from the conclusion that the only texture variance was not sufficient to segregate all the landcover features in the study area, this method was not carried out for further analysis.

5.2.3. Option 3: classification based on colour and texture

This study was intended to identify the vegetation sub-classes to remove the trees, bushes and crops from the DSM. The first approach based on colour could broadly differentiate vegetation and non-vegetation classes and the second approach based on texture of landcover features could only differentiate the vegetation sub-classes. The combined approach was done to utilise both the properties of landcover features.

Classification on orthophoto with 0.25m spatial resolution

Supervised classification was carried out on texture variance image of orthophoto in 6 different window sizes using maximum likelihood classifier. The classification results are shown in Figure 5-1 for the part of study area depicted in Figure 4-7. Different window sizes were used to find out the most suitable size to classify the area.

Table 5-2 Overall accuracy and k-statistics of the classification results on colour- texture orthophoto in different window sizes

Window	3 X 3	11 X 11	27 X 27	35 X 35	43 X 43	71 X 71
Overall accuracy	28%	52%	54%	54%	50%	48%
K	0.06	0.367	0.436	0.408	0.313	0.34

From the classification results it was observed that with window of 3 X 3 (Figure 5-1A) the variation in texture was not recognised in homogeneous areas such as forest and meadows. Moreover due to overlap in the texture character among different landcover classes most of the features were classified as buildings and roads. With increase in the window size the class segregation improved. However with a window 71 X 71 (Figure 5-1F) the texture information were generalised, which again resulted in misclassification. This fact is also supported by the classification accuracies obtained by error matrix and kappa statistics and they area presented in Table 5-2.

The overall accuracies of the window 27 X 27 and 35 X 35 were found to be the same (54%). However the k-statistics for the former was better. Therefore, in deciding the most suitable window size for this classification the k value was considered. In this regard it should be noticed that though among all different window sizes 27 X 27 window offer the best classification result (Appendix F2), still it was inferior with respect to that obtained using colour only. The reason behind this selection was that both the user's accuracy (81.2%) and the producer's accuracy (81.2%) for crop/bush/tree class in the classification of colour-texture orthophoto using 27 X 27 window was found to be much better than that obtained using colour only (42.2% and 60.9% respectively) (Table 5-3).

Table 5-3 Error matrix for classification results of orthophoto (0.25m) based on colour and texture using 27 X 27 window

Classified data	**Reference data**						
	Crop / bush / tree	**Meadow**	**Building / road**	**Bare agri-land**	**Bare land / sand**	**Water**	**Sum**
Crop/bush/tree	**13**	3	0	0	0	0	16
Meadow	0	**4**	0	0	0	0	4
Building/ road	3	3	**3**	4	0	0	13
Bare agri-land	0	2	0	**5**	0	0	7
Bare land/ sand	0	4	0	2	**0**	2	8
Water	0	2	0	0	0	**0**	2
Sum	16	18	3	11	0	2	50
Producer's accuracy	81.2%	22.2%	100	45.5%	-	100%	
User's accuracy	81.2%	100%	23%	71.4%	-	25%	

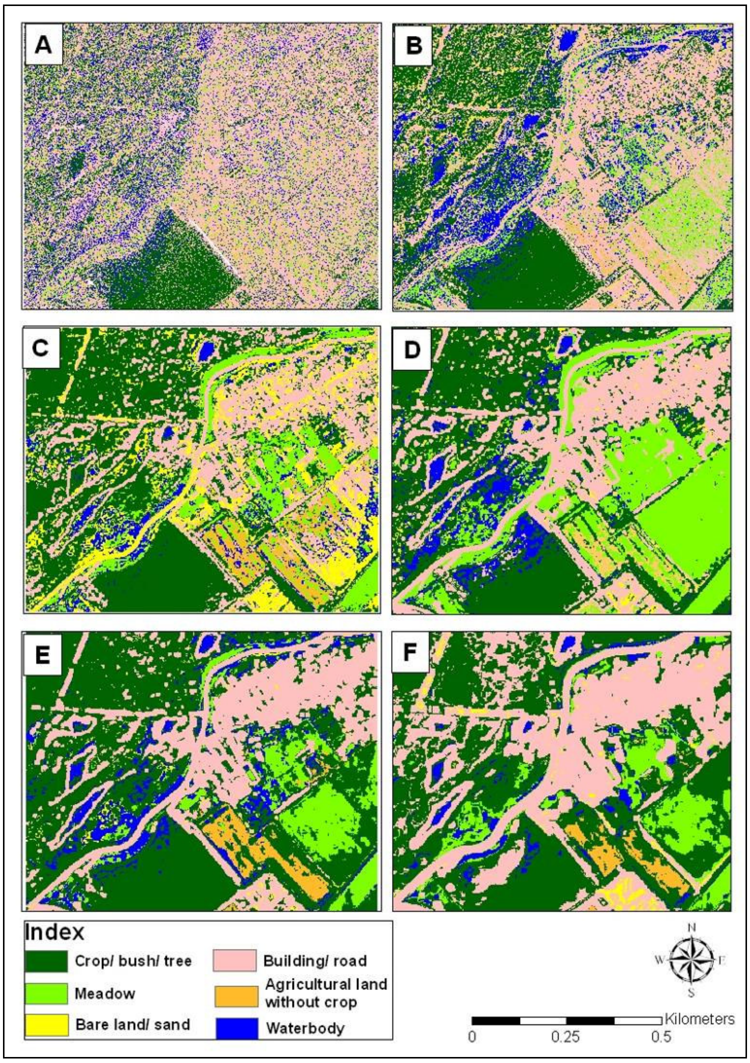

Figure 5-1 Supervised classification on colour orthophoto (0.25m) with texture variance in (A) 3 X 3 window, (B) 11 X 11 window, (C) 27 X 27 window, (D) 35 X 35 window, (E) 43 X 43 window and (F) 71 X 71 window sizes.

<u>Classification on orthophoto with 5m spatial resolution</u>

The classification on the 5m orthophoto (Appendix F3) was done on the basis of 10 training classes for each class. The classification accuracies are provided in Table 5-4.

The accuracy assessment depicted that majority of the crop/tree/bush and meadow classes were classified correctly. However, there were quite misclassification among sand and building/road classes. The Overall accuracy of this classification was better than that carried out considering only colour of landcover features. The same was true for kappa coefficient. This indicates the improvement in feature identification process when both colour and texture were considered. Increase of user's accuracy indicated decrease in error of commission. Moreover, this classification was performed on orthophoto with 5m cell resolution where the information on the photo gets generalised to some extent. In spite of that classification accuracy had increased and this indicated that combining colour and texture of landcover feature can improve the classification efficiency substantially.

Table 5-4 Error matrix for classification results of orthophoto (5m) based on colour and texture using 3 X 3 window

Classified data	Reference data						
	Crop/ bush/tree	**Meadow**	**Building/ road**	**Bare agri-land**	**Bare land/ sand**	**Water**	**Sum**
Crop/bush/tree	**27**	3	1	0	0	1	32
Meadow	1	**45**	0	2	0	1	49
Building/ road	4	2	**10**	1	11	5	33
Bare-agri land	3	7	0	**8**	0	1	
Bare land/ sand	3	4	2	1	**13**	5	28
Water	2	6	1	2	2	**25**	38
Sum	40	67	14	14	27	37	199
Producer's accuracy	67.5%	67.2%	71.4%	57.1%	48.1%	67.6%	
User's accuracy	84.3%	91.8%	30.3%	42.1%	46.4%	65.7%	
Overall accuracy						64.32%	
k						63	

The orthophotos of two different spatial resolutions were also classified into two classes (vegetation and non-vegetation) to be used in the neighbourhood analysis. In both the cases the overall accuracy and k statistics were 94% and 0.934 respectively.

5.3. Feature removal

From the classification process described above two different classified data were obtained.

1. Classified orthophoto (0.25m) on the basis of colour and texture.
2. Classified orthophoto (5m) on the basis of colour and texture.

Two different methods were used for feature removal from the derived DSM, which are

- binarisation and interpolation
- neighbourhood analysis

Both the feature removal methods were carried for the two classified images.

5.3.1. Binarisation and interpolation

The crops, bushes and trees were removed using the method described in section 4.3.3. The stepwise development of the method is shows in the Figure 5-3 for a small part of the study area (Figure 5-2). The same process was performed for orthophoto with 5m resolution.

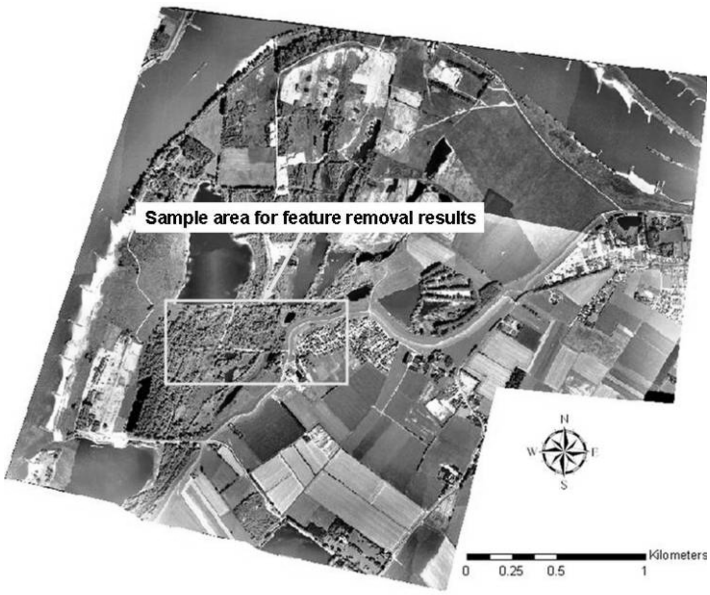

Figure 5-2 Map showing the sample area in gray colour orthophoto for feature removal results.

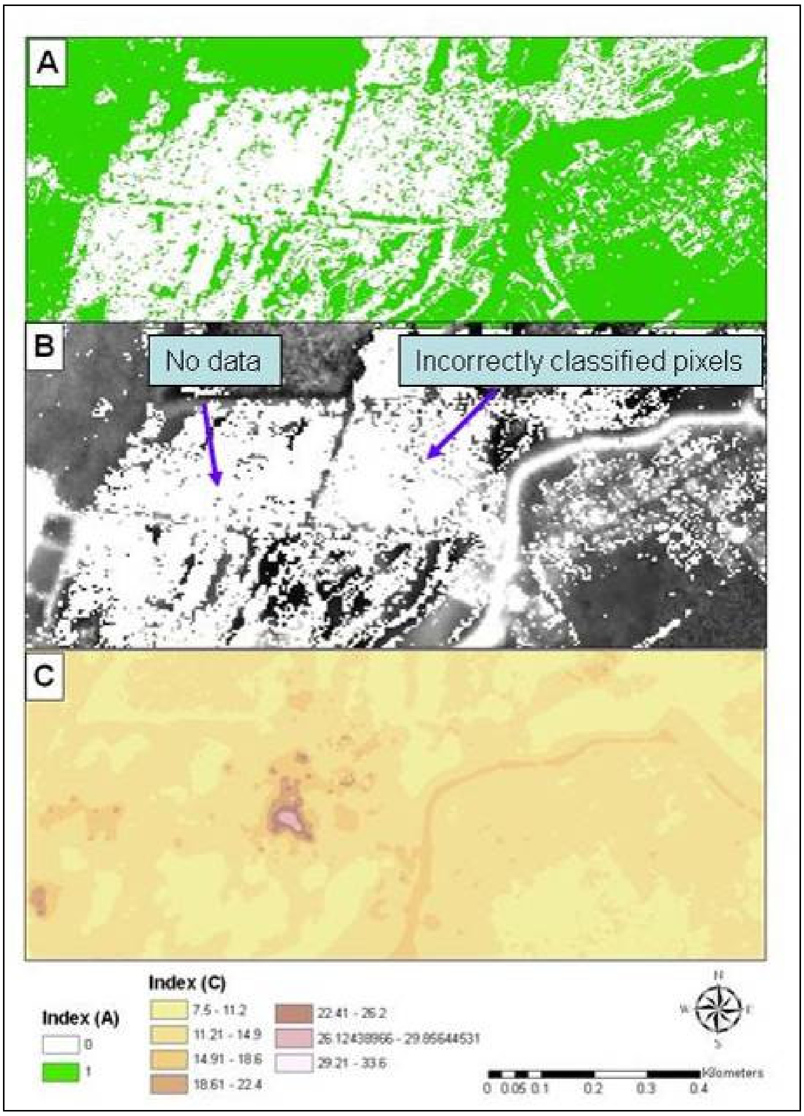

Figure 5-3 Different steps of binarisation and interpolation method: (A) binary image of classified orthophoto (0.25m), (B) DSM without crop/bush/tree class obtained by multiplying binary image with the DSM, (C) the pseudo-DTM obtained after interpolation.

5.3.2. Neighbourhood analysis

The neighbourhood analysis was performed with both the classified image. A stepwise development of the method using orthophoto with 5m spatial resolution is shown in Figure 5-4 for a small part of the study area depicted in Figure 5-2. Same procedure was carried out using the orthophoto with 0.25m spatial resolution.

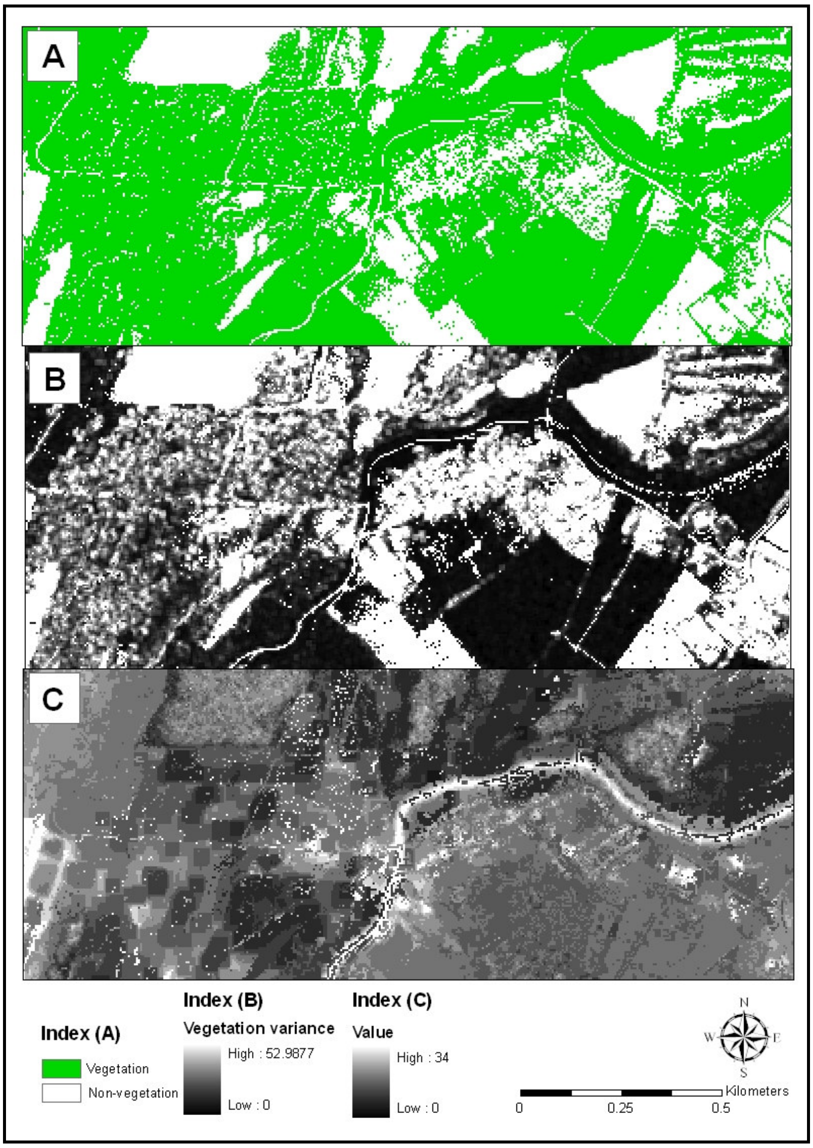

Figure 5-4 Different steps of neighbourhood analysis method: (A) Binary image of orthophoto classified in to two classes (vegetation and non-vegetation), (B) texture variance image of the vegetation obtained by multiplying binary image with the texture variance image, (C) the pseudo-DTM obtained after neighbourhood analysis

5.4. Accuracy assessment of the pseudo-DTM

For qualitative assessment of the efficiency of the feature removal methods the changes in the height of the derived pseudo-DTMs from the DSM was calculated. Figure 5-5 shows the locations with crop/bush/tree landcover class in the study area. Figure 5-6 depicts the change detection maps for a small part of the study area annotated by a box in Figure 5-5. In the areas with crop/bush/tree landcover class the height of the surface was supposed to reduce in the pseudo-DTM.

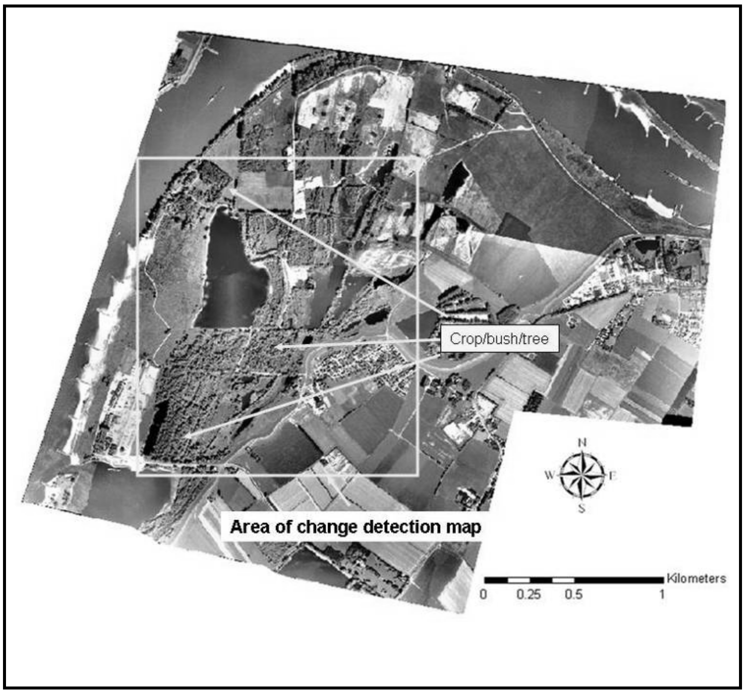

Figure 5-5 Orthophoto (0.25m) of the study area with crop/bush/tree location

Quantitatively, accuracy assessment on the derived pseudo-DTMs was carried out using two different methods. Firstly the LiDAR DTM was subtracted from the DSM and each of the pseudo-DTMs. The mean and standard deviation of the residuals were calculated. Table 5-5 shows the error statistics of the DSM and the pseudo-DTMs with respect to the LiDAR DTM.

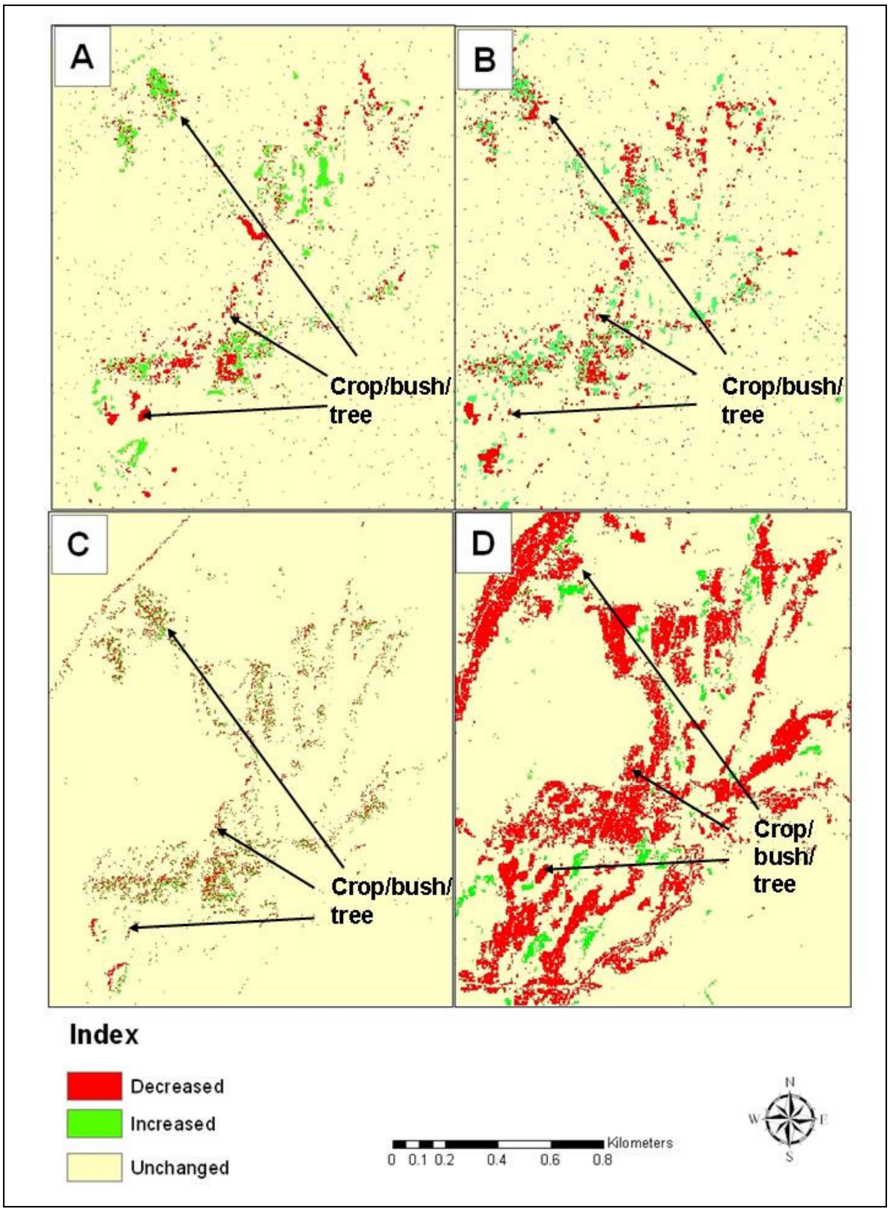

Figure 5-6 Change detection maps for pseudo-DTM obtained by (A) binarisation and interpolation method for 0.25m orthophoto, (B) binarisation and interpolation method for 5m orthophoto, (C) neighbourhood analysis method for 0.25m orthophoto and (D) neighbourhood analysis method for 5m orthophoto

Table 5-5 Error estimation of the DSM and the pseudo-DTMs with respect to the LiDAR DTM

Data 1	Data 2	Min (m)	Max(m)	Mean (m)	SD (m)
DSM	L-DTM	-17.020	30.209	6.595	13.714
P-DTM (BI_25cm)	L-DTM	-16.190	25.722	4.766	12.170
P-DTM (BI_5m)	L-DTM	-17.000	28.527	5.763	13.220
P-DTM (NA_25cm)	L-DTM	-17.390	27.902	5.256	12.152
P-DTM (NA_5m)	L-DTM	-17.500	24.834	3.667	12.293

P-DTM (BI_25cm) = pseudo-DTM derived from the orthophoto of 25cm spatial resolution using binarisation and interpolation method.
P-DTM (BI_5m) = pseudo-DTM derived from the orthophoto of 5m spatial resolution using binarisation and interpolation method.
P-DTM (NA_25cm) = pseudo-DTM derived from the orthophoto of 25cm spatial resolution using neighbourhood analysis.
P-DTM (NA_5m) = pseudo-DTM derived from the orthophoto of 5m spatial resolution using neighbourhood analysis.
SD = standard deviation

In the second level accuracy assessment difference images were generated only for the areas with crops, bushes and trees. The results are shown in Table 5-6.

Table 5-6 Error estimation of the pseudo -DTM respect to the LiDAR DTM in areas with corps, bushes and trees

Data 1	Data 2	SD (m)
P-DTM (BI_25cm)	L-DTM	10.46
P-DTM (BI_5m)	L-DTM	12.99
P-DTM (NA_25cm)	L-DTM	13.25
P-DTM (NA_5m)	L-DTM	9.28

6. Discussion

6.1. Introduction

The main objective of this study is to generate a suitable surface model for flood risk assessment. In this regard the study is carried out to identify and delineate the surface features on the available data set and then on the basis of their spatial extension they have been removed from the DSM. This chapter will provide an in depth assessment of the methodological approach on the basis of data available and different practical scenario, comparative quality assessment of the results, the sources of errors and finally applicability of the method in flood risk assessment.

6.2. The methodological approach

The method is designed to move through two different phases which are (i) identification of different surface features and (i) removal of relevant surface features from the DSM.

6.3. Feature identification: classification results

The identification of features was performed using supervised classification with maximum likelihood classifier. The available data set for this step was the orthophoto of the study area and the properties of the features that are used for the classification are colour and texture as the data does not contain any spectral information. Poor classification results were obtained while using only colour for classification. Overlapping texture statistics of different landcover features identified in the study area. Thus methods using these variables individually are rejected. The integrated colour-texture approach was carried out in two ways, one of which used them as single entity, while the other as separate entities.

However, it is clear from the error matrices and the kappa statistics of different classification results (Table 5-3 and 5-4) that none of the methods is universally applicable. Although several studies were carried out in classification based on texture of landcover features (Caridade *et al.*, 2008, Gong *et al.*, 1992, Lovan *et al.*, 2007, Hudak and Wessman, 1998, Ge *et al.*, 2006, James *et al.*, 2006) they differ from the present study either in the data type or in composition of the study area. For example James *et al.* (2006) used LiDAR data along with the aerial photo to improve the classification. Likewise, the use of different vegetation indices along with texture for multispectral aerial photo can improve the classification accuracy (Lovan *et al.*, 2007). The classifier algorithm also has an effect on the classification result and this was proved by Caridade *et al.* (2008). They used three different classifier namely Euclidean classifier, Mahalanobis classifier and Bayes classifier to classify vegetation sub-classes in aerial photo and could attain a considerable accuracy in classification results. The data available for this study is scanned aerial photo with only colour information in three layers (blue, green and red). No spectral information is available for this study. The study area is consisted of heterogeneous landcover features which show overlapping colour and texture pattern. The vegetation sub-classes e.g. trees, bushes, crops and grasses appear in the shades of same colour (Figure 4-3). Similarly, some building roofs, agricultural lands without crop, bare ground and roads sometime appear in same colour (Figure 4-4). Same can be found for water, shadows and some buildings with black roofs. Moreover, the brightness of same landcover features varies with different camera and sun angles during photo acquisition, which is another source of classification error. The orthophoto was generated from two strips of overlapping stereo photos which differ in the brightness and colour for same landcover feature (Figure 6-1). All these problems ultimately lead to the misclassification of some landcover features.

Figure 6-1 Map showing the colour difference of same landcover feature

Moreover, high spatial resolution of the orthophoto is also a source of error in the classification, which is also admitted in the study by Caridade *et al.* (2006). They found the classification accuracy to increase substantially with reduced image resolution. This is also true for the present study which shows an improvement in the overall accuracy and kappa when the orthophoto with 5 m spatial resolution is used instead of 0.25m (Table 5-3 and 5-4). In high resolution images the uncertainty in feature identification arises due to same signature pattern of different class. The effect of shadow is also very prominent, which also increases the uncertainty in the classification. In addition to this low resolution data needs comparatively less computation time than the high resolution data. Obviously, the choice of resolution of the data depends on the purpose of the end users.

In another classification the texture and colour is used separately. It was concluded in a study by Maenpaa and Pietikainen (2004) that only in static or same illumination condition the colour information in texture can improve the classification accuracy while in varying illumination condition the gray scale texture can perform better. The source data for this study was generated from the stereo pairs which were captured from the aircraft which views the same location from two different angles generating varying illumination condition. This leads to intra-class variation according to colour and brightness and it is also a source of error in classification. The effect is more prominent when the images come from two different stripes. To avoid this problem the orthophotos could be classified separately and mosaiced later on for further analysis but when there is variation of colour and texture for same landcover class this method do not reduce the uncertainties. The texture statistics were calculated using ENVI 4.5 software. One major problem which was experienced during texture calculation is that the process took long computation time (7-8 hours) to calculate only one texture statistics (variance) for all three layers of the orthophoto together. The file size for each texture image is also vey large (~ 2 GB) to handle easily. Thus in the second type of classification, colour was used to identify vegetation and non-vegetation features (above 90% overall accuracy) and then gray scale texture variance was further used to classify vegetation sub-classes.

6.4. Discussion on feature removal methods

Two methods that were adopted to remove the crops, bushes and trees identified from classification are (i) binarisation and interpolation and (ii) neighbourhood analysis.

Figure 5-6 shows the map describing the change in height in the pseudo-DTM after the correction routine applied on the DSM. The change detection map highlights the areas where the height is changed (decreased or increased) after correction process. Although the feature removal methods are only supposed to reduce the height of the areas with crop/ bush/ tree class, the height of some areas is found to increase in the pseudo-DTM obtained by both the methods. This behaviour can be explained from the error in classification. The classified image on the basis of colour and texture together was used as the main input of this method. Both overall accuracy and kappa are not very good for the classification results (Table 5-3 and 5-4) which implies both omission and commission errors are high. Thus, in the first method, when the classified images were binarised many pixels that actually belongs to crop/bush/tree class were retained and vice versa. Moreover, pixels of crop/ bush/ tree class which are not correctly classified still maintained their height on the pseudo-DTM. Thus during interpolation the surrounding height of such pixels has increased (Figure 6-2).

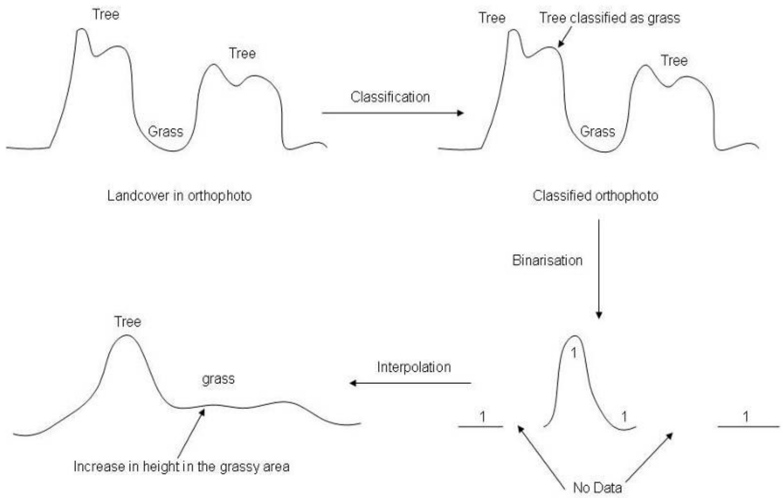

Figure 6-2 Misclassification leading to increase in height in pseudo-DTM

The estimated error (Table 5-6) in the areas with error class (tree, bush and crop) using binarisation and interpolation method is still much high after correction process, which indicates that the method could not remove the error classes from the DSM. Although the errors calculated in Table 5-6 for the neighbourhood analysis method are comparatively less than that calculated in Table 5-5 because of not accounting for the effect of non-error classes (such as buildings and roads). The binarisation and interpolation method was demonstrated by James *et al.* (2006) who successfully carried out the method resulting in an elevation model with very low standard deviation (0.23m) with respect to the ground measurements. However, James and his colleagues used both multispectral aerial photo and LiDAR data to identify the surface features which is actually more effective rather than using scanned colour aerial photo only. Morphological dilation was also used in their study to include any misclassified pixels in the transitional area, but this buffering may lead to inclusion of wrong pixels i.e. pixels from other landcover classes which should not be removed, especially in areas with heterogeneous landcover. It is important to notice that in both the pseudo-DTM (with 0.25m and 5m orthophoto) the elevation of some parts of the area has increased with respect to the DSM which is not expectable. The reason behind is again the misclassification of landcover features.

The second approach to remove the crops, bushes and trees was the neighbourhood analysis. According to the statistical values (Table 5-6) and the change detection images (Figure 5-6) this method could remove more trees bushes and crops compared to binarisation and interpolation method. The major positive point of this method is that it differentiates the tall and short vegetations only according to their texture variance which well segregate these two landcover classes. However, the change detection map (Figure 5-6D) shows the decrease in height in the areas with meadows along with the areas with trees, bushes and crops. In some of those areas the texture of meadows are quite similar to that of trees. That is why in the neighbourhood analysis the matrix could not segregate the meadows and the trees. This analysis performs better when orthophoto with 5m resolution is used instead of 0.25m because of the resolution conflict between the classified orthophoto and the DSM. The neighbourhood analysis is mainly used for the LiDAR data in several researches successfully (Zhang *et al*., 2003a, Chen *et al.*, 2007, Koch *et al.*, 2006) as it can segregate the ground and non-ground points from the return pulses, which is not available in the data used in present study. However, inclusion of spectral information with the texture can further improve the correction process using neighbourhood analysis. As the input data of the feature removal process in both the methods are classified data, it is essential to ensure good classification of the data to identify the features correctly. Otherwise, error in feature identification propagates through the different steps of the feature removal process resulting in erroneous output.

Comparing the Figure 5-6 A, B, C and D, it is very clear that the neighbourhood analysis method can remove more crop/ bush/ trees from the DSM than the binarisation and interpolation method when the spatial resolution of the orthophoto is 5m. This is also supported by the accuracy assessment of the pseudo-DTM (Table 5-6). However, there is no such considerable difference in the derived pseudo-DTMs using binarisation and interpolation method and neighbourhood analysis method when the orthophoto of 0.25m resolution is used for the classification. The reason is the conflict between the different resolution of the classified orthophoto and the DSM which are 0.25m and 5m respectively.

The neighborhood analysis method is better than the other method with respect to another aspect. While capturing a stereo pair using aerial photography, the camera is viewed at different angles. Therefore, while creating a DSM a smooth surface over those features are generated with an overestimation of the actual area of the landcover feature. The sharp edges of the landcover features are not depicted accurately and the shape of feature is not retained as it is. This error ultimately induces error in the pseudo-DTM. However, in neighborhood analysis this error can also be avoided provided the data is classified accurately.

Thus from this background, the methodology followed in neighbourhood analysis agrees with the alternate hypothesis of the research (section 1.4) that it is possible to identify and remove the impermeable obstacles to water flow effectively from photogrammetrically derived DSM. The effectiveness of the method can be improved by providing more detailed dataset.

6.5. Justification of the methods in different scenario

Three different scenarios were developed in chapter 4. In one of the classification methods the colour and texture of the image were used as a complimentary variable whereas in the other they were used as separate entity. It is necessary to assess the methods in the context of the different scenarios. While using colour and texture together, in an area with distinct boundary and spatial characteristics among the landcover features as case 1 scenario (Figure 4-11) the classification can work well. On the other hand in an area with case 2 scenario (Figure 4-12) the presence of mixed landcover classes decreases the classification accuracy. The error matrices in Table 5-3 and 5-4 show that the land cover classes has overlapping colour and texture signature pattern among different classes. For this reason in such scenario, this classification method can not identify the landcover features correctly. In case 3 scenario (Figure 4-13 and Appendix E1), if the vegetation on the hump or the depression is homogeneous the classification method will identify the features correctly, while the presence of mixed classes they can not be identified correctly.

On the other hand in neighbourhood analysis method the classification was performed considering colour and the texture of features separately. As the vegetation classes have distinct colour than the other classes, they could be classified satisfactorily. However, with the very high resolution image (0.25m spatial resolution) this the accuracy of classification can decrease due to the presence of shadows in the vegetated areas. The masking out of the non-vegetated class from the texture variance image reduces the chance of misclassification of the vegetation class to other non-vegetation classes. As the meadows and the tall vegetations have distinct texture characteristics this classification method should work satisfactorily for all the three scenarios. In this study this method also leads to some misclassification because of the different illumination condition and different texture pattern for the same class in different areas.

If we consider the feature removal process for different scenario different output will be encountered. In this regard it is necessary to keep in mind that all the results from feature removal process depend on how accurately the features are identified on the images. To assess only the efficiency of the feature removal methods let us suppose that all the features are correctly classifies in the first instance. Therefore, for the simplest case 1 scenario, in a flat area with respect to elevation (Figure 4-11) both the feature removal methods should work well. For the binarisation and interpolation method the accurately classified areas with trees, bushes and crops will be converted to “NoData” in the DSM after which the data gap will be filled with interpolation from the surrounding height values. In a flat area interpolation is also much easier than that in undulating terrain. In the case 2 scenario (Figure 4-12) if the terrain is flat this method will work satisfactorily. However, the method fails in the case 3 scenario (Figure 4-13). One of the constraints of the input data is that it is not possible to identify the terrain under the landcover features. Thus the understory hump or depression in the terrain will be converted to the flat terrain using binarisation and interpolation method. If there is an open end of the hump or depression with out any landcover feature on it then it can be recognisable by this method. In neighbourhood analysis method similar results are expected if the texture descriptors can differentiate the vegetation sub-classes accurately. In that situation the in case 1 and case 2 scenarios this method should work satisfactorily. However in case 3 scenario if the extent of the hump or depression is less than the extent of the scanning window, the terrain will be flattened. In this regard it is very important be conscious in deciding the size of the scanning window which can vary in different areas.

However, the feature removal process is not very simple from the DSM which is generated from aerial photographs. As the DSM is generated from the pairs of stereo photos, the occlusion effect is very high in the DSM. It does not depict clear edges of the landcover features rather generates a smooth surface overestimating the height of terrain in the occluded areas. Thus it is important to notice that how these occluded areas are classified, which ultimately affect the efficiency of the removal process.

6.6. Implication of the results in flood risk assessment

The aim of this improvement of the elevation model is to make it suitable for further flood risk assessment. As one of the main inputs of the flood models the elevation information should be the very accurate. The level of accuracy, obviously, depends on the intensity of flood events as well as the purpose of the study. With a very high intensity flood the vertical error of ±1m in elevation model may not have much affect but for low intensity map ±30 cm error can have significant impact in obstructing water flow. Different scenarios discussed in chapter 4 are important to review in this regard. Especially, in case 3 scenario (Figure 4-13) the presence of a hump or depression under vegetation is not accurately characterised by the methods. Therefore, for example, if there is a dike with the vegetation on the top of it, it is necessary to estimate the accurate height of that area. Otherwise, if by the correction routine they are eliminated, the efficiency of flood prediction will also be affected. From the results it is quite clear that the pseudo-DTMs obtained by the binarisation and interpolation method can not be used further for flood risk assessment. Although, among the results obtained from neighbourhood analysis the pseudo-DTM from the orthophoto with 5 m resolution has the lowest RMSE, still the error is much higher to be used in detailed flood risk assessment. The flood models sometimes are very sensitive to very small changes in the topography and that can affect the model prediction.

As the pseudo-DTMs are derived in very high resolution, it is always a matter of question how much it is plausible to use a detailed elevation model in flood prediction. With a very detail elevation model, the flood model will need very high computation time as well as computer memory. For a wider floodplain this is really a problem. Moreover, it is also necessary to ensure that a flood model is programmed to handle detail elevation information. If the requirement of the flood model is a 30m elevation model, there is hardly any need of generating 5m elevation model. Reducing the detail in elevation model will automatically reduce the error in it. Some times the model input of elevation data is substantially different from the source elevation data. This results in the generalisation of the detailed information such as dikes and other flow obstacles.

6.7. Summary

The chapter provides an assessment of the methodological approach used for this study. It also discuss about the sources of errors in the results. The transferability of the method has been discussed with respect to different scenarios. Lastly, the chapter focuses briefly on the implication of the results in flood risk assessment.

7. Conclusions and Recommendations

The elevation model is one of the main components which are used in flood models for flood risk assessment. In this regard proper characterization of the elevation model is necessary. Automatically generated elevation model includes all the surface features on it and is known as DSM. From the perspective of flood modelling, at a definite scale of flood, it is necessary to identify relevant surface features which act as permeable blockage to water flow and remove them from the surface model to generate a pseudo-DTM. This study has developed a methodological approach to identify the features on the DSM and remove them from it. The surface model is created from stereo pairs of aerial photo. The orthophoto is used for identification of features and a reference LiDAR DTM is used to estimate the errors in the derived pseudo-DTM. Based on the research questions the specific conclusions are summarised below:

7.1. Specific Conclusions

1. **The relevant artifacts that should be removed from the DSM to generate the pseudo- DTM.**

   The study area is consisted of 5 main landcover features which are man-made features, vegetation, agricultural area, water body and bare ground or sand. Among them water body and bare grounds do not pose any obstruction to water flow. The nature of obstruction depends on the flood intensity. For medium and low intensity flood man-made features such as buildings, dikes and embankments acts as impermeable obstacles to water flow (Frazão *et al.*, 2004, Mignot *et al.*, 2005). The role of vegetation in such condition is different. For instance, except the meadows, the trees, bushes and tall crops act as permeable obstacles to water flow. No doubt, these vegetation sub-classes pose a friction to water flow which is usually represented as roughness coefficient in flood models, but they do not block the water flow. Water can easily pass through the areas with trees, bushes and crops. Only the velocity of water flow changes in this area from that in the open areas. However in the surface model those areas are depicted as impermeable blockage to water flow. Therefore, it is necessary to remove the trees, bushes and tall crops from the surface model while retaining the others for better flood prediction and flood risk assessment for medium and low intensity flood event.

2. Formulation of semi-automatic method to generate pseudo-DTM by removing the relevant artifact from the DSM

Two different methodological approaches are used in this study to identify the surface features and remove the relevant features from the DSM. The colour and texture of the orthophoto is used to identify the landcover features. Binarisation and interpolation and neighbourhood analysis are used to remove the trees, bushes and tall crops from the DSM. It has been found that the binarisation and interpolation method can not perform well with the available data. The neighbourhood analysis method can perform better than the other method and it is most effective when the spatial resolution of the orthophoto is same as the DSM. Thus with the available data set the neighbourhood analysis is a better method, specifically for this area, which can generate pseudo-DTM semi-automatically by removing relevant surface features from the DSM. However, in the simplest scenario the method works well. Use of multispectral data, LiDAR data and object oriented classification can further improve the method.

3. Vertical accuracies of the derived pseudo-DTM

The vertical accuracies of the derived pseudo-DTMs are calculated by comparing the heights of the same locations in the pseudo-DTMs and in the LiDAR DTM for areas with trees, bushes and tall crops. In the other areas the surface height is compared with that of the DSM. For the areas with trees, bushes and crops the highest accuracy (lowest SD) is achieved for the pseudo-DTM obtained from the neighbourhood analysis using orthophoto with 5m resolution. For the other pseudo-DTMs the vertical accuracy is very poor. However, for the areas with meadow and buildings the vertical accuracy is good enough for all the derived DTMs.

7.2. Limitations of the Research

1. The ground control points for triangulation method were collected from the existing LiDAR DTM and orthophoto which have some inherent vertical and horizontal errors in it. These errors are ultimately induced in the derived elevation model.

2. As the surface model is developed from the stereo pairs of aerial photo strong occlusion effect is present in the surface model, which is a common problem of photogrammetrically derived surface models. This error affected the further feature identification and removal process.

3. The source data of the orthophoto is scanned multispectral aerial photo which does not contain any spectral information. This property of the source data has limited the applicability of the potential methods for feature identification and removal.

4. In the source data same landcover features are captured with different illumination which results in the intra-class variation in colour and texture. This leads to poor classification accuracy.

5. Both the feature removal processes using orthophoto with 0.25m resolution suffer resolution conflict with the DSM which has 5m grid spacing. The spatial information orthophoto with 5 m resolution becomes much generalised to be classified accurately and thus also produce erroneous result.

6. In the neighbourhood analysis the only texture of the landcover features has been considered to decide the threshold to segregate the meadows from trees, bushes and tall crops. In some places the texture signature of those features overlaps due to error in the source data.

7. The variation of spatial resolution of the available data is one of the main reasons for the failure of the methods in some cases. It would have been a good analysis if both the orthophoto and the DSM are obtained in fine resolution (0.25m). Using LPS it was not possible to generate a DSM with 0.25m spatial resolution. LPS can generate DSM up to 1.25m spatial resolution.

8. The validation of the pseudo-DTMs has not been done due to time constraint. A simulation using the derived pseudo-DTMs in flood model could predict the efficiency of the method and sensitivity of the flood model with changing surface conditions.

7.3. Recommendations

The research has provided a methodological approach to generate pseudo-DTM by identifying the surface features and removing the relevant features from the DSM. On the basis of the research methodology and the limitations of the research the following recommendations are proposed for the future scope of the study.

1. It is necessary to collect the ground control points before developing the DSM to minimise the error in source data for further analysis on it.

2. The use of digital aerial photo instead of scanned photo can improve the classification accuracy and the efficiency of classification using spectral properties of landcover features. Moreover, with the very high resolution data the object oriented classification can be more useful than pixel based method.

3. The neighbourhood analysis can be further improved by incorporating more criteria (instead of texture only) to segregate meadows from trees, bushes and crops.

4. It is necessary to analyse the effects of uncertainties and errors in the classification in flood risk assessment. In this regard it is also necessary to identify the optimum resolution of the source data to maximise the efficiency of the method.

5. Further research can also be carried out in finding the nature of obstruction of different surface features at different spatial resolution of the input data and how it affects the flood risk assessment and flood management.

Finally, the author wishes to conclude by mentioning that it is very important to develop the most suitable surface model for flood risk assessment by minimising the uncertainties. In this regard it is necessary to identify accurately the obstacles and non-obstacle surface features to generate the pseudo – DTM by removing the non-obstacle features and retaining the others. The above research proposes a methodological approach for this purpose, which is a stepping stone for the further research in this subject. Considering the above recommendations along with limitations of the available data and the methodology, the study generates further scope of research to improve the method for efficient flood risk assessment.

References:

Alkema, D. (2007) *Simulating floods: on the application of a 2D hydraulic model for flood hazard and risk assessment*. Thesis (Ph.D), ITC, Enschede.

Baillard, C., Dissard, O., Jamet, O. & Maitre, H. (1998) Extraction and textural characterization of above-ground areas from aerial stereo pairs: a quality assessment. *ISPRS Journal of Photogrammetry & Remote Sensing* 53, 130-141.

Bates, P. D., Horritt, M. S., Smith, C. N. & Mason, D. (1997) Integrating remote sensing observations of flood hydrology and hydraulic modelling. *Hydrological Processes*, 11, 1777-1795.

Baltsavias, E. P. (1996) Digital ortho-images -- a powerful tool for the extraction of spatial- and geo-information. *ISPRS Journal of Photogrammetry and Remote Sensing,* 51, 63-77.

Brivio, P.A., Colombo, R., Maggi, M. & Tomasani, R. (2002) Integration of remote sensing data and GIS for accurate mapping of flooded areas. *International Journal of Remote Sensing,* 23, 429-441.

Burrough, P. A. & Mcdonnel, R. A. (1998) *Principles of geographical information systems.* Oxford etc., Oxford University Press, 98 - 160.

Caelli, T. & Reye, D. (1993) On the classification of image regions by colour, texture and shape. *Pattern Recognition,* 26, 461-470.

Caridade, C. M. R., Maracal, A. R. S. & Mendonaca, T. (2008) The use of texture for image classification of black & white air photographs. *International Journal of Remote Sensing*, 29, 593-607.

Carlisle, B. H. (2005) Modelling the Spatial Distribution of DEM Error. *Transactions in GIS*, 9, 521-540.

Chen, Q., Gong, P., Baldocchi, D. & Xie, G. (2007) Filtering airborne laser scanning data with morphological filtering. *Photogrammetric Engineering and Remote Sensing,* 73, 175 - 185.

Choi, Y., Park, H. D. & Sunwoo, C. (2008) Flood and gully erosion problems at the Pasir open pit coal mine, Indonesia: a case study of the hydrology using GIS. *Bulletin of Engineering Geology and the Environment,* 67, 251-258.

Chow, V. T. (1964) *Handbook of Applied Hydrology,* 1st Ed. New York, McGraw-Hill Book Company, 25-26.

Chow, V. T., Maidment, D. R. & Mays, L. W. (1988) *Applied Geology,* New York, McGraw-Hill Book Company, 1-17.

Coburn, C. A. & Roberts, A. C. B. (2004) A multiscale texture analysis procedure for improved forest stand classification. *International Journal of Remote Sensing*, 25, 4287-4308.

Cord, M., Jordan, M., Cocquerez, J. P. & Paparoditis, N. (1999) Automatic extraction and modelling of urban buildings from high resolution aerial images. *International Archives of Photogrammetry and Remote Sensing,* 32, 187–192.

CRED (2005) Disasters in numbers. (Online available) http://www.unisdr.org/disaster-statistics/pdf/2005-disaster-in-numbers.pdf , (accessed on: August 18, 2008).

CRED (2007) Disasters in numbers. (Online available) http://www.unisdr.org/eng/media-room/facts-sheets/2007-disasters-in-numbers-ISDR-CRED.pdf , (accessed on: August 18, 2008).

CRED/EM-DAT: Emergency events database. (Online available) http://www.emdat.be/Database/terms.html , (accessed on: September 18, 2008).

ERDAS (2008) Leica Photogrammetric Suit Project manager: User's guide. Atlanta, ERDAS.

Falkner, E. (1995) *Aerial Mapping, Methods and Applications,* 1st Ed. London, Lewis Publishers, 1-7.

Fisher, P. F. & Nicholas, J. T. (2006) Causes and consequences of error in digital elevation models. *Progress in Physical Geography,* 30**,** 467-489.

Forte, F., Strobl, R. & Pennetta, L. (2006) A methodology using GIS, aerial photos and remote sensing for loss estimation and flood vulnerability analysis in the Supersano-Ruffano-Nociglia Graben, southern Italy. *Environmental Geology,* 50, 581-594.

Franklin, S. E., Hall, R. J., Moskal, L. M., Maudie, A. J. & Lavigne, M. B. (2000) Incorporating texture into classification of forest species composition from airborne multispectral images. *International Journal of Remote Sensing*, 21, 61-79.

Frazão, S. S., Noël, B. & Zech, Y. (2004) Experiments of dam-break flow in the presence of obstacles. (Online available) http://scholar.google.co.uk/scholar?hl=en&q=Experiments%20of%20dam-break%20flow%20in%20the%20presence%20of%20obstacles&um=1&ie=UTF-8&sa=N&tab=ws , (accessed on: September 18, 2008).

Garcia, M. A. & Puig, D. (2007) Supervised texture classification by integration of multiple texture methods and evaluation windows. *Image and Vision Computing,* 25, 1091-1106.

Ge, S., Carruthers, R., Gong, P. & Herrera, A. (2006) Texture analysis for mapping Tamarix parviflora using aerial photographs along the Cache Creek, California. *Environmental Monitoring and Assessment,* 114, 65-83.

Gong, P., Marceau, D. J. & Howarth, P. J. (1992) A comparison of spatial feature extraction algorithms for land-use classification with SPOT HRV data. *Remote Sensing of Environment,* 40, 137-151.

Gong, J., Li, Z., Zhu, Q., Sui, H. & Zhou, Y. (2000) Effects of various factors on the accuracy of DEMs: an intensive experimental investigation. *Photogrammetric Engineering and Remote Sensing,* 66 (9)**,** 1113-17.

Green, C. H., Parker, D. J. & Tunstall, S. M. (2000) Assessment of flood control and management options, options assessment: IV.4, *In: Flood Hazard Research Centre*, Middlesex University, 42-50.

Hinz, S. & Baumgartner, A. (2003) Automatic extraction of urban road networks from multi-view aerial imagery. *ISPRS Journal of Photogrammetry & Remote Sensing,* 58, 83– 98.

Horritt, M. S. & Bates, P. D. (2002) Evaluation of 1D and 2D numerical models for predicting river flood inundation. *Journal of Hydrology,* 268, 87-99.

Hudak, A. T. & Wessman, C. A. (1998) Textural analysis of historical aerial photography to characterize woody plant encroachment in South African Savanna - II. real digital images. *Remote Sensing of Environment,* 66, 317-330.

Hutchinson, M. F. & Gallant, J. C. (2000) *Digital Elevation Model and Representation of Terrain Shape,* New York etc., John Wiley & Sons, Inc.

IPCC (2007) Climate change 2007: synthesis report. (Online available) http://www.ipcc.ch/pdf/assessment-report/ar4/syr/ar4_syr.pdf (accessed on: September 17, 2008).

Itaya, A., Miura, M. & Yamamoto, S. I. (2004) Canopy height changes of an old-growth evergreen broad-leaved forest analyzed with digital elevation models. *Forest Ecology and Management,* 194, 403-411.

James, T. D., Barr, S. L. & Lane, S. N. (2006) Automated correction of surface obstruction errors in digital surface models using off-the-shelf image processing. *The Photogrammetric Record,* 21, 373-397.

Jensen, J. R. (1996) *Introductory Digital Image Processing: A Remote Sensing Perspective,* 2nd Ed., *New* Jersey, Prentice Hall, 187 - 192.

Kasser, M. & Egels, Y. (2002) *Digital photogrammetry,* 1st Ed., London, Taylor & Francis, 159 - 292.

Kenward, T., Lettenmaier, D. P., Wood, E. F. & Fielding, E. (2000) Effects of digital elevation model accuracy on hydrologic predictions. *Remote Sensing of Environment,* 74**,** 432-444.

Kerle, N. (2002) Volume estimation of the 1998 flank collapse at casita volcano, Nicaragua: a comparison of photogrammetric and conventional techniques. *Earth Surface Processes and Landforms,* 27, 759–772.

Knudsen, T. (2005) Technical note: pseudo natural colour aerial imagery for urban and suburban mapping. *International Journal of Remote sensing,* 26, 2689-2698.

Koch, B., Heydar, U. & Weinacker, H. (2006) Detection of individual tree crown in airborne Lidar data. *Photogrammetric Engineering and Remote Sensing,* 72, 357 - 363.

Koukoulas, S. & Blackburn, G. A. (2005) Mapping individual tree location, height and species in broadleaved deciduous forest using airborne LIDAR and multi-spectral remotely sensed data. *International Journal of Remote sensing,* 26, 431-455

Lillesand, T. M. & Kiefer, R. W. (2002) *Remote Sensing and Image Interpretation,* 4th Ed., Singapore, John Wiley & Sons, Ltd., 568-575.

Lindsay, J. B. & Creed, I. F. (2006) Distinguishing actual and artefact depressions in digital elevation data. *Computers & Geosciences,* 32, 1192-1204.

Liu, X. (2008) Airborne LiDAR for DEM generation: some critical issues. *Progress in Physical Geography,* 32, 31-49.

Longley, P. A., Goodchild, M. F. , Maguire, D.J., Rhind, D.W. (2005) *Geographic Information Systems and Science*, 2nd Ed. Chichester, John Wiley & sons, Ltd.

Lovan, C., Boldo, D. & Cord, M. (2007) Automatic extraction of urban vegetation structures from high resolution imagery and digital elevation model. *In: Urban Remote Sensing Joint Event,* April11-13*, Paris*, France.

Lu, Y. H., Trinder, J. C. & Kubik, K. (2006) Automatic building detection using the dampster-shafer algorithm. *Photogrammetric Engineering and Remote Sensing,* 72, 395-403.

Maenpaa, T. & Pietikainen, M. (2004) Classification with color and texture: jointly or separately? *Pattern Recognition,* 37, 1629-1640.

Maidment, D. R. (1993) *Handbook of Hydrology,* 1st Ed. New York, McGraw-Hill Inc., 21.1 - 21.35.

Marks, K. & Bates, S. P. (2000) Integration of high-resolution topographic data with floodplain flow models. *Hydrological Processes,* 14, 2109-2122.

Mason, D. C., Horritt. M.S., Hunter, N. M. & Bates, P. D. (2007) Use of fused airborne scanning laser altimetry and digital map data for urban flood modelling. *Hydrological Processes*, 21, 1436–1447

Massalabi, A., Dong-chen, H., Benie, G. B. & Beaudry, E. (2004) Detecting information under and from shadow in panchromatic Ikonos images of the city of Sherbrooke. *In: Geoscience and Remote Sensing Symposium, 2004. IGARSS '04. Proceedings. 2004 IEEE International, 20-24 September, 2004, Anchorage, AK, 2000-2003.*

Maune, D. F. (2001) *Digital Elevation Model Technologies and Applications: The DEM Users Manual,* 1st Ed., Maryland, American Society of Photogrammetry and Remote Sensing, 1-23.

Mignot, E., Paquier, A. & Haider, S. (2005) Modeling floods in a dense urban area using 2D shallow water equations. *Journal of Hydrology*, 327, 186– 199.

Mikhail, E. M., Bethel, J. S. & Mcglone, J. C. (2001) *Introduction to Modern Photogrammetry,* 1st Ed., New York, John Wiley & Sons, Inc., 9-12.

Mohamed, M. A. & Kim, K. E. (2003) Use of texture filters to improve quality of digital elevation models derived from stereo imagery. *In: Geoscience and Remote Sensing Symposium, 2003. IGARSS '03, Proceedings. 2003 IEEE International*, *21-25 July, 2003*, *VA, USA.*

Munich Reinsurance (2007) Natural catastrophes 2007 comparison with previous years. (Online available) http://www.munichre.com/app_resources/pdf/press/press_releases/2007/2007_12_27_app2_en.pdf*, (accessed on:* August 18, 2008).

Nasset, E. (2002) Determination of Mean Tree Height of Forest Stands by Digital Photogrammetry. *Scandinavian Journal of Forest Research,* 17, 446-459.

Oksanen, J. & Sarjakoski, T. (2005) Error propagation of DEM-based surface derivatives. *Computers and Geosciences*, 31, 1015-1027.

Peters, D. L., Prowse, T. D., Pietroniro, A. & Leconte, R. (2006) Flood hydrology of the Peace-Athabasca Delta, northern Canada. *Hydrological Processes*, 20, 4073-4096.

Portmann, F. T. (1997) Hydrological runoff modelling by the use of remote sensing data with reference to the 1993-1994 and 1995 floods in the river Rhine catchment. *Hydrological Processes,* 11, 1377-1392.

Priestnall, G., Jaafar, J. & Duncan, A. (2000) Extracting urban features from LiDAR digital surface models. *Computers, Environment and Urban Systems,* 24, 65-78.

Profeti, G. & Macintosh, H. (1997) Flood management through LANDSAT TM and ERS SAR data: a case study. *Hydrological Processes,* 11, 1397-1408.

Rango, A. & Anderson, A. T. (1974) Flood hazard studies in the Mississippi river basin using remote sensing. *JAWRA Journal of the American Water Resources Association*, 10, 1060-1081.

Rees (2000) The accuracy of Digital Elevation Models interpolated to higher resolutions. *International Journal of Remote Sensing,* 21, 7-20.

Ryherd, S. & Woodcock, C. (1996) Combining spectral and texture data in the segmentation of remotely sensed images. *Photogrammetric Engineering and Remote Sensing,* 62, 181-194.

Sali, E. & Wolfson, H. (1992) Texture classification in aerial photographs and satellite data. *International Journal of Remote Sensing,* 13, 3395-3408.

Samadzadegan, F., Azizi, A., Michael, H. & Lucas, C. (2005) Automatic 3D object recognition and reconstruction based on neuro-fuzzy modelling. *ISPRS Journal of Photogrammetry & Remote Sensing,* 59, 255-277.

Sanyal, J. & Lu, X. X. (2004) Application of remote sensing in flood management with special reference to monsoon Asia: a review. *Natural Hazards,* 33, 283-301.

Sithole, G. & Vosselman, G. (2003) Comparison of filtering algorithms. *In: ISPRS Commission III WG3.* Dresden, Germany.

Smith, M. J., Smith, D. G., Tragheim, G. & Holt, M. (1997) Shorter contributions Dems and ortho-images from aerial photographs. *The Photogrammetric Record,* 15, 945-950.

St-onge, B., Vega, C., Fournier, R. A. & Hu, Y. (2008) Mapping canopy height using a combination of digital stereo-photogrammetry and lidar. *International Journal of Remote Sensing,* 29, 3343 - 3364.

Turner, H. & Steiner, D. (1979) Digital image processing techniques to extract metric data on buildings from shadows on simulated air photos. *Photogrammetria,* 35, 141-160.

UNESCO (2008) Climate change. (Online available) http://portal.unesco.org/science/en/ev.php-URL_ID=6154&URL_DO=DO_TOPIC&URL_SECTION=201.html , *(accessed on:* September 18, 2008).

van der Sande, C. J., Dejong, S. M. & Deroo, A. P. J. (2003) A segmentation and classification approach of IKONOS-2 imagery for land cover mapping to assist flood risk and flood damage assessment. *International Journal of Applied Earth Observation and Geoinformation,* 4, 217-229.

Veregin, H. (1997) The effects of vertical error in digital elevation models on the determination of flow-path direction. *Cartography and Geographic Information Science,* 24, 67-79.

Vosselman, G. (2000) Slope based filtering of laser altimetry data. IAPRS, *Working group III / 2*, vol. XXXIII, Amsterdam.

Waser, L. T., Ecker, K., Ginzler, C., Küchler, M., Schwarz, M. & Thee, P. (2006) Extraction of forest parameters in a mire environment using airborne spectral data and digital surface models. *In*: *Workshop on 3D Remote Sensing in Forestry.14-15 February, 2006, Vienna*.

Wechsler, S. P. (2007) Uncertainties associated with digital elevation models for hydrologic applications: a review. *Hydrology and. Earth System Sciences,* 11, 1481–1500.

Wheeler, P. J., Kunapo, J., Peterson, J. A. & Mcmahon, M. (2007) Mapping relative inundation vulnerability of land parcels on low-lying ground: exemplification with a photogrammetrically-derived DEM-based models of lakes entrance, Victorial, Australia. *In: Proceedings of the Spatial Science Institute Biennial International Conference (SSC2007), 14-15 May, 2007, Hobart, Tasmania, Australia,* 902 - 915

Wise, S. M. (2000) Assessing the quality for hydrological applications of digital elevation models derived from contours. *Hydrological Processes,* 14, 1909 - 1929.

Wise, S. M. (2007) Effect of differing DEM creation methods on the results from a hydrological model. *Computers & Geosciences* 33, 1351-1365.

Wu, R. S., Shih, D. S., Li, M. H. & Niu, C. C. (2008) Coupled surface and ground water models for investigating hydrological processes. *Hydrological Processes,* 22, 1216-1229.

Wulder, M. A., Ledrew, E. F., Franklin, S. E. & Lavigne, M. B. (1998) Aerial image texture information in the estimation of northern deciduous and mixed wood forest leaf area index (LAI) - I. scene models and simulated images. *Remote Sensing of Environment,* 64, 64-76.

Zebedin, L., Klaus, A., Gruber-geymayer, B. & Karner, K. (2006) Towards 3D map generation from digital aerial images. *ISPRS Journal of Photogrammetry and Remote Sensing,* 60, 413-427.

Zhang, K., Shu-ching, C., Whitman, D., Mei-ling, S., Jianhua, Y. & Chengcui, Z. (2003a) A progressive morphological filter for removing non-ground measurements from airborne LIDAR data. *In: IEEE Transactions on Geoscience and Remote Sensing,* 41, 872-882.

Zhang, Q., Wang, J., Gong, P. & Shi, P. (2003b) Study of urban spatial patterns from SPOT panchromatic imagery using textural analysis. *International Journal of Remote Sensing,* 24, 4137-4160.

Appendices:

Appendix A1: Number of flood events and the most devastating floods in last two decades in different continents (CRED/EM-DAT).

Continents	No. of floods (2000-2008)	No. of floods (1990-1999)	Most devastating flood		
			Location (year)	Total Affected	Damage (Million US $)
Europe	219	112	Germany (2002)	330000	11600
Asia	554	354	China (1998)	24000000	30000
America	259	180	Mexico (2007)	1600000	30000
Africa	332	152	Mozambique (2000)	4500000	419
Australia & New Zealand	22	19	Victoria and New South Wales (Australia) (1993)	20530	4.9

Appendix B1: Theory behind GLCM used to calculate different texture parameters (Jensen, 1996).

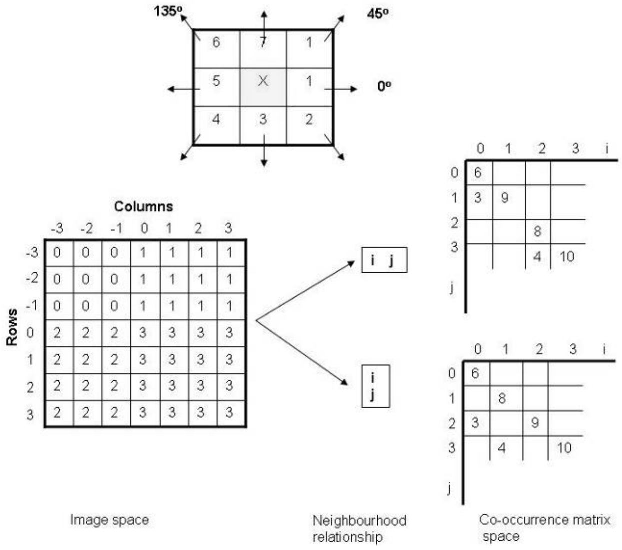

Appendix B2 : Effect of scanning resolution on DEM height accuracy (Smith *et al*., 1997).

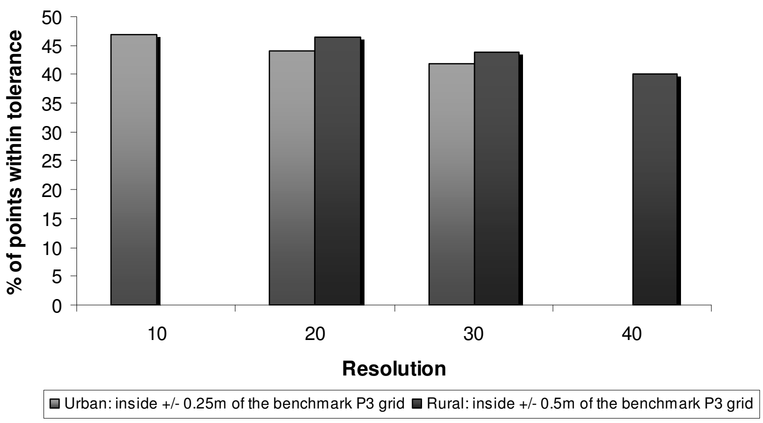

Appendix B3: Interpolation

The ***IDW*** interpolation method applies Tobler law for estimation of the elevation of unknown points on the basis of the weighted average of the known measurements. The weight is calculated with respect to the distance of the point with unknown elevation from that with known elevation. Many different ways are there for calculating weight but the most common method calculates the weight as the inverse square of the distance ($w_i = 1/d^2$). In areas with peaks and pits this method fails. The interpolation using the ***thiessen polygon*** is based on the concept of nearest neighbourhood. The point with unknown elevation is assigned an elevation value of the nearest point. This leads to an elevation map in which each point with known elevation is surrounded by a close polygon known as thiessen polygon inside which the elevations are same at all points. In ***spline*** two dimensional cubic polynomials are fitted locally through an area with some point of unknown elevation. The curve is usually fitted through a small number of data points and the joints between one part of the curve with the other is continuous. ***Kriging*** is based on geostatistics and semi-variogram. It uses statistical method [Z(x) = m(x) + e'(x) + e''] to describe a continuous surface. It counts the structural component [m(x)], the locally varying component which is called the residuals [e'(x)] as well as the spatially independent error (e'') during interpolation. The m(x) is determined using a trend surface. To determine e'(x), the data is detrained and interpolation is done on the residual assuming a spatial autocorrelation between known and unknown points. Kriging is one type of weighted average (considers both distance and angle between known and unknown points) which assumes that sum of all weight is 1 and the weights are optimised to minimise the uncertainty in estimation (Burrough and McDonnell, 1998, Longley, 2005).

Appendix B4: The effect of modelling method on the accuracy of DEM in different terrain type (Gong, 2000).

Method	**Flat area**		**Hilly area**		**Mountainous area**	
	No. of GP	**RMSE (m)**	**No. of GP**	**RMSE (m)**	**No. of GP**	**RMSE (m)**
Random to grid	152	1.52	83	1.18	41	3.77
TIN	152	1.20	83	1.12	41	2.94

Appendix B5: Accuracy (%) of DEM in different landcover types (Smith *et al.*, 1997).

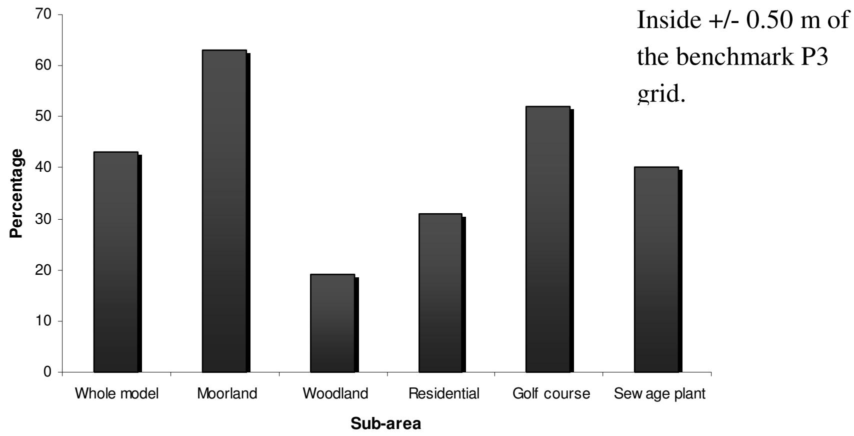

Appendix C1: Different errors present in the DTM file derived from LiDAR data (Product Specification AHN 2000).

Terrain type	RMSE (m)	Systematic error (m)	Dot point density
Beach, dune and inter-tidal zone	0.15	+/-0.05	1 per 1 m^2
Lawn, short grass	0.15	+0.05	1 per 16 m^2
Helm vegetation, natural grassland	0.20	+0.20	1 per 16 m^2
Salt marsh with dense vegetation , areas with dense shrub vegetation (the magazine), Reed vegetation, agriculture crops	0.20	Height of vegetation	1 per 16 m^2
Areas with dense shrub vegetation (without leaves)	0.20	+0.20	1 per 16 m^2
Hard, flat topography	0.15	+0.05	1 per 16 m^2
Woodland	0.20	+0.10	1 per 36 m^2

Appendix C2: Camera Calibration Details

CAMERA TYPE: RMK TOP 30
LENS TYPE: Topor A3
MAX. APERTURE: F/5.6
NON FOCAL LENGTH: 305 MM
CALIBRATED FOCAL LENGTH:305.571 mm
FIDUCIAL MARKS (used for interior orientation of the aerial photos)

X_1	-112.990 (mm)	Y_1	-0.010 (mm)
X_2	-112.995 (mm)	Y_2	-0.012 (mm)
X_3	-0.002 (mm)	Y_3	112.985 (mm)
X_4	-0.004 (mm)	Y_4	-113.007 (mm)
X_5	113.003 (mm)	Y_5	112.989 (mm)
X_6	-112.996 (mm)	Y_6	-113.014 (mm)
X_7	-112.994 (mm)	Y_7	112.993 (mm)
X_8	112.985 (mm)	Y_8	-113.008 (mm)

Appendix D1: Map showing the DSM of the total area using 11 stereo pairs.

Appendix D2: Algorithms of statistical descriptors of texture available in ENVI 4.5 used to analyse the orthophoto.

1. Among the first order statistic descriptors average, standard deviation and entropy were used.

$$\textit{Average} = 1/W \sum_{i=0}^{q_k} i \times f_i \quad \text{(i)}$$

$$\textit{Variance} = 1/W \sum_{i=0}^{q_k} (i - AVG)^2 \times f_i \quad \text{(ii)}$$

$$\textit{Entropy} = \sum_{i=0}^{q_k} f_i /W \ln f_i /W \quad \text{(iii)}$$

f_i = frequency of gray level occurring in a pixel window
q_k = quantization level of band k (e.g $= 2^8 = 0$ to 255)
W = total number of pixel in a window (Jensen, 1996).

2. Among the second order statistical texture descriptor angular second momentum, contrast, correlation, dissimilarity and homogeneity were used.

The angular second momentum defines the local uniformity of gray level.

$$\textit{Angular Second Momentum} = \sum_{i=0}^{q_k} \sum_{j=0}^{q_k} h_c(i, j)^2 \quad \text{(iv)}$$

Contrast describes the local variation of gray level.

$$\textit{Contrast} = \sum_{i=0}^{q_k} \sum_{j=0}^{q_k} (i - j)^2 \times h_c(i, j)^2 \quad \text{(v)}$$

Homogeneity describes the compactness of distribution of gray level.

$$\textit{Homogeneity} = \sum h_c(i, j) / [1 + (i - j)^2] \quad \text{(vi)}$$

Dissimilarity is same as contrast but increases linearly with contrast.

$$\textit{Dissimilarity} = \sum h_c(i, j) * \mathrm{abs}(i - j) \quad \text{(vii)}$$

$h_c(i, j)$ = Probability of the pixel with gray level (i, j) separated by the distance c.

Appendix D3: Frequency distribution of texture angular second momentum of meadow and crop/bush/tree class.

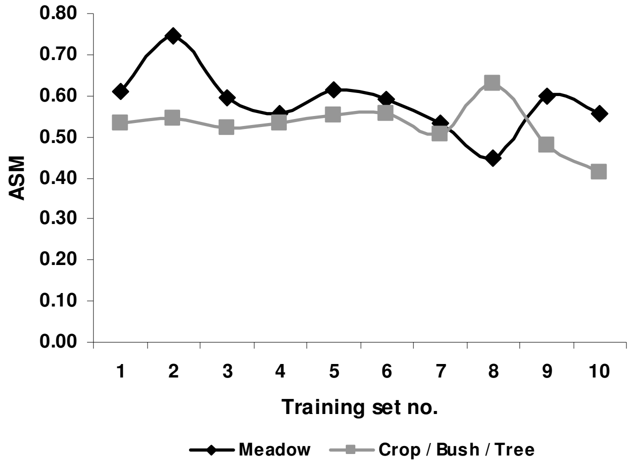

Appendix D4: Frequency distribution of texture dissimilarity of meadow and crop/bush/tree class.

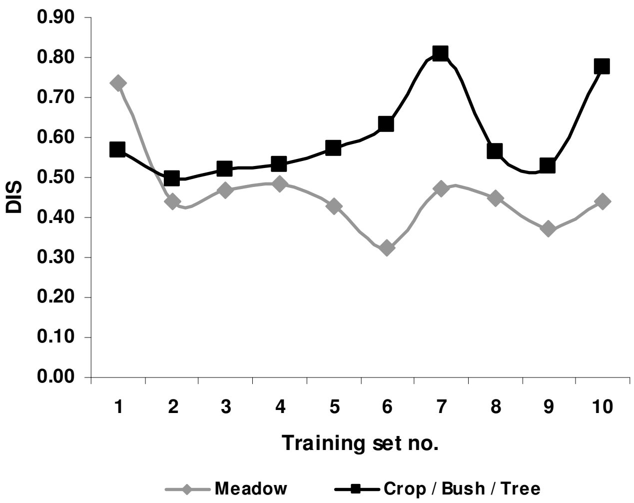

Appendix D5: Frequency distribution of texture homogeneity of meadow and crop/bush/tree class.

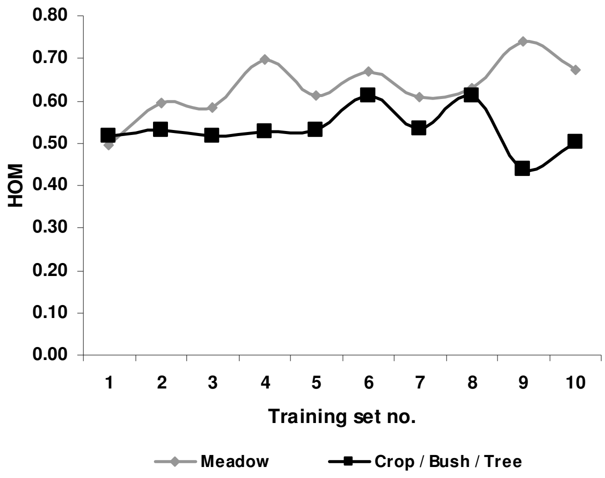

Appendix D6: Frequency distribution of texture mean of meadow and crop/bush/tree class.

Appendix D7: Frequency distribution of texture entropy of meadow and crop/bush/tree class.

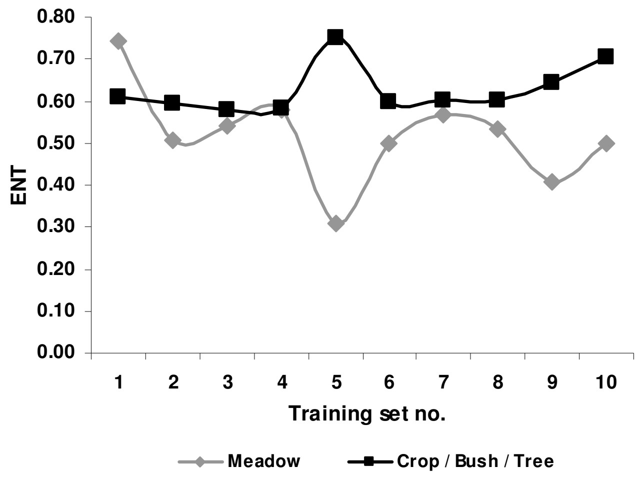

Appendix D8: Frequency distribution of texture contrast of meadow and crop/bush/tree class.

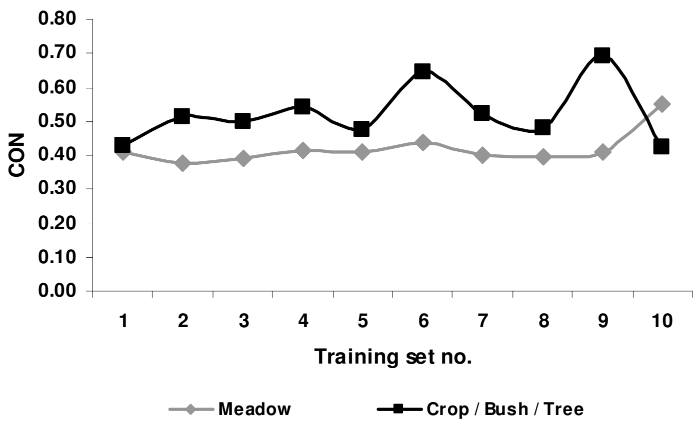

Appendix E1: Depression under vegetation (as seen in field photograph) leads to error in the resulting pseudo – DTM generated by binarisation and interpolation method.

Appendix F1: Texture variance of landcover features in a part of the study area (0.25 m resolution orthophoto) with (A) 3 X 3 window, (B) 11 X 11 window, (C) 27 X 27 window, (D) 35 X 35 window, (E) 43 X 43 window and (F) 71 X 71 window.

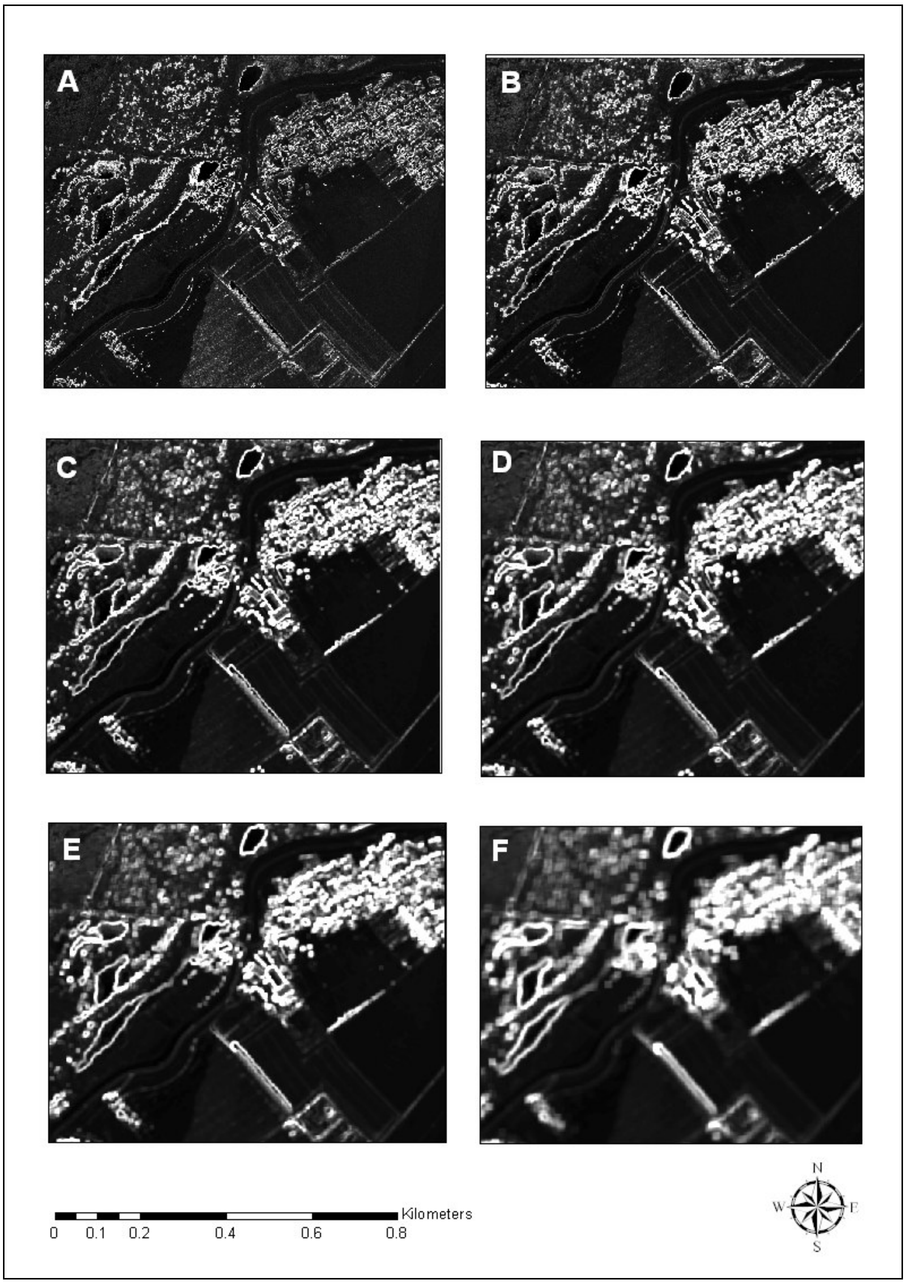

Appendix F2: Classified orthophoto (0.25m) on the basis of colour and texture in window 27 X 27.

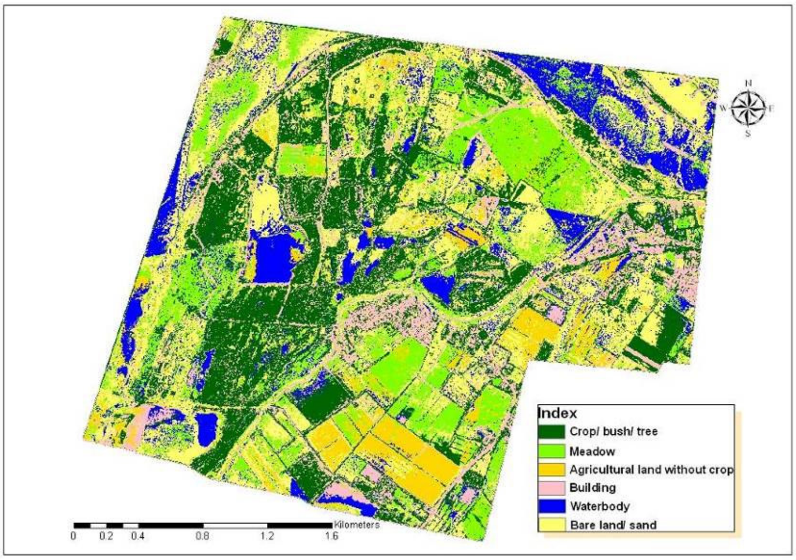

Appendix F3: Classified orthophoto (5m) on the basis of colour and texture in window 3X3.